# The Impact of Spatial Resolution on Land Cover Mapping: A Small Watershed Case Study

**By**

**Emily Clarvit**

**Department of Environmental Science**

**Allegheny College**

**Meadville, Pennsylvania**

**April, 2022**

**Submitted in fulfillment of the senior thesis requirements of the**

**Department of Environmental Science at Allegheny College**

**and approved by the senior thesis committee.**

| | | | |
|---|---|---|---|
| Chris Shaffer | 4/11/22 | | 4/11/22 |
| **Prof. Chris Shaffer** | **Date** | **Dr. Jesse Swann-Quinn** | **Date** |

Emily S. Clarvit

**Pledge**

## Table of Contents


**Table of Contents** **ii**

**Acknowledgements** **iii**

**Abstract** **iv**

**Introduction** **1**

**Methods** **5**

*Study Region* **5**

*Data Sources* **7**

*Data Manipulation* **8**

*Data Analysis* **8**

**Results** **15**

**Discussion** **19**

**References** **24**

**Appendix** **31**

**Acknowledgements**

First of all, I would like to thank my senior thesis advisor, Chris Shaffer, for his assistance through every part of this project. He introduced me to this research topic, answered my many questions, and tolerated my constant visits during his office hours. I would have been unable to complete this project without his help. I also would like to thank Jesse Swann-Quinn for his help as my second reader. Additionally, I want to thank the rest of the Environmental Science and Sustainability Department for helping me to find something I feel truly passionate about. Every professor here has provided me with so much knowledge and helped me to hone valuable skills that I know will benefit me throughout my life. I am so thankful that I chose to complete my undergraduate studies here at Allegheny.

To my mom and dad, thank you for always supporting me in all of my endeavors. I wouldn't be the person I am today without your love and guidance. Thank you for reading drafts of this project and listening to my concerns at all hours of the night. Your care and encouragement have been invaluable during this project and throughout my college career as a whole.

I would also like to thank all of my friends, both here at college and back at home, for all of their kindness and support. Without you, I wouldn't have taken the time to stop and enjoy my senior year. All of you are amazing people who constantly inspire me and bring joy to my life.

Name: Emily Clarvit Date: April, 2022
Major: Environmental Science and Sustainability
Thesis Committee: Professor Chris Shaffer, Dr. Jesse Swann-Quinn

Title: The Impact of Spatial Resolution on Land Cover Mapping: A Small Watershed Case Study

**Abstract**

Terrestrial remote sensing, the contactless recording of electromagnetic radiation via film or sensors mounted on airborne or spaceborne platforms, can be used in the creation of land cover data. Image classification is the process of assigning meaning to raw spectral data by identifying different features and separating them into informational classes. In this study, supervised, object-based classification was utilized to create fine resolution land cover data for a subset of small watersheds in northwestern Pennsylvania. This land cover data was compared to data obtained from the National Land Cover Database, which has a much coarser resolution, in order to examine differences between the two, determine where potential misclassifications occur, and assess which method is a more accurate and efficient option. Error matrices were utilized to verify the accuracy of each image classification, resulting in an average accuracy of 96.6%. The differences in the percentage of natural cover, agriculture, and developed land in the classified images and the National Land Cover Database were calculated and averaged, with the largest differences occurring in the developed category. Overlay analysis was utilized to further examine how much the two data sources differed. Only 14.5% of the pixels classified as developed by the National Land Cover Database received the same classification in the classified images, with 80% receiving a different classification. This tendency of the National Land Cover Database to overrepresent developed land could influence decision making in various studies that rely on having accurate land cover data. Although additional effort is required, image classification may represent a more accurate method of obtaining land cover data for use in large-scale watershed analysis.

## Introduction

Terrestrial remote sensing, defined as the non-contact detecting and recording of electromagnetic radiation (e.g., visible light, infrared light, microwave) by way of cameras and sensors mounted on suborbital and orbital platforms and the visual and digital analysis of this radiation, is an incredibly valuable tool for mapping the landscape (Campbell & Wynne, 2011, p. 6). Categories include aerial photography, satellite data, light detection and ranging (LIDAR), and much more. Remote sensing is a cost-effective tool that can provide information on both large and small scales (Khatami et al., 2016). Remotely sensed data can be used to study land change across an entire continent or simply to determine the land cover composition of one small watershed (Khatami et al., 2016). Additionally, it can be utilized for a variety of applications, including forest monitoring, meteorology and climatology, medical science, geology, natural hazard detection, and biodiversity studies (Khatami et al., 2016; Weng, 2012, p. 8).

Beginning in the 1930s, cameras mounted on aircraft were the first remote sensing method that was used to study the landscape. Photographs are produced by recording the light reflectance of various objects and landscape features on film (Morgan et al., 2010). Film is coated with layers of photographic emulsion, which is made of light-sensitive silver halide crystals that react differently depending on the reflectance of the features being photographed (Morgan et al., 2010). Aerial photographs are capable of recording electromagnetic radiation over the wavelength range of 0.3 to 0.9 micrometers; this includes ultraviolet, visible, and near-infrared light (Weng, 2012, p. 50). The interpretation of aerial photographs involves identifying different objects or features in the photographs (Weng, 2012, p. 80). Tone, color, size, shape, texture, pattern, shadow, and association are all utilized to distinguish different objects in an aerial photograph (Morgan et al., 2010; Weng, 2012, p. 80). Landscape features like deep, calm water absorb most light, making them appear dark in tone (Minnesota IT Services, n.d.). In natural color photos, vegetation appears green because it reflects green light while absorbing red and blue light (Knipling, 1970). In color-infrared photos, vegetation is a bright red or pink, as plants also reflect a great deal of infrared light (Knipling, 1970; Minnesota IT Services, n.d.). Color-infrared photos are captured using a yellow filter to block blue light and three different emulsion layers to record green, red, and infrared light (Weng, 2012, p. 77). Conversion from hardcopy to digital via optical scanning can allow film-based aerial photographs to be used digitally, however there is a significant loss of detail. Once identified, different objects can be digitized manually in geographic information systems (GIS). Digitization is the process of delineating groups of homogeneous pixels by tracing locations, pathways, and boundaries. An alternate approach would be to utilize multispectral digital photographs rather than traditional film-based photos. Advantages of digital aerial photography include immediate image access, reusable digital storage, and an ability to record positional data (Morgan et al., 2010). Digital aerial photography became more prevalent in the 1990s when digital cameras became more widely available to the public (Morgan et al., 2010).

Aerial photographs are very effective for mapping small ecosystems and are a vital source of historical landscape data (Morgan et al., 2010). Unfortunately, there are also drawbacks to using aerial photographs to study the landscape. Manual interpretation of aerial photographs, whether on paper or in GIS, is often time consuming, subjective, and not cost effective (Morgan et al., 2010).

Current trends employ sensors mounted on aircraft, drones, and satellites. Satellite imagery is obtained through the use of electro-optical sensors, which receive and measure radiance from the ground as electrical signals and convert these signals into numerical values called digital numbers (Weng, 2012, p. 122). Electro-optical sensors have several advantages over the silver halide crystals used in film-based aerial photography. Digital numbers provide exact reflectance values, providing more precise information than what can be obtained from a traditional aerial photograph (Weng, 2012, p. 122) Additionally, these sensors have a larger spectral range, extending into the reflected infrared and thermal infrared regions (Weng, 2012, p. 122). Electro-optical sensors also have broad spatial and temporal coverage and can be used continuously, making satellite imagery and digital aerial photography more cost effective than traditional aerial photography (Morgan et al., 2010). One example of satellite-based remote sensing is the Landsat Program. Since 1972, NASA and the USGS have collaborated to launch 9 different satellites, on which increasingly advanced sensors were mounted (Loveland & Dwyer, 2012; NASA, 2022). The goal of the program is to obtain multispectral imagery of the earth's surface in order to monitor change and effectively manage resources for economic and environmental purposes (Loveland & Dwyer, 2012). Landsats 8 and 9 are currently active, recording light in the visible, near-infrared, shortwave-infrared, and thermal-infrared spectrums (NASA, 2022). Despite the convenience of programs like Landsat, there are also several disadvantages to satellite imagery. As a more recent technology, satellite imagery cannot provide historical data from before the 1970s, while the earliest aerial photographs date back to the 1930s (Morgan et al., 2010). Another limitation of satellite imagery is the fact that the spatial resolution of most of this imagery is coarser than that of aerial photographs, meaning that less detail is provided (Cleve et al., 2008; Morgan et al., 2010). Although satellite imagery sources like SPOT, IKONOS, QuickBird, and WorldView can provide higher resolution data, these sources are not available for free like Landsat (Morgan et al., 2010).

Historically, manual interpretation was the only way to analyze remotely sensed data. In recent decades, new techniques have been developed to improve the efficiency and accuracy of image interpretation. Digital image analysis is a process that allows for the detection and identification of features in remotely sensed images by computers (Weng, 2012, p. 189). Different features in imagery have different spectral responses, meaning they reflect and absorb different amounts of energy at different wavelengths (DiBiase, n.d.; Weng, 2012, p. 204). These different spectral response characteristics are represented by a unique combination of digital numbers for each pixel (Weng, 2012, p. 204). Beginning

in the 1980s, various image classification techniques have been developed (Li et al., 2014). Image classification is a type of image analysis that uses these digital numbers and special algorithms to classify pixels into different spectral classes (Weng, 2012, p. 204). Each pixel in an image is assigned to a different informational class based on its spectral signature (e.g., water, forests, agricultural land). Land cover classification is an especially important use as it has many applications in various sectors; examples include policy development, hydrology modeling, ecosystem services, natural resource management, and much more (Saah et al., 2019).

One application of land cover data is watershed analysis. Studies focused on sedimentation, eutrophication, and creating indices of biotic integrity all rely on having accurate land cover data. Some studies have examined the connection between land cover type within a watershed and soil erosion and sedimentation. Excessive sedimentation is often a consequence of runoff and is considered a nonpoint source pollutant (Nicklow & Muleta, 2001). Sediment pollution can reduce water quality as well as disrupt aquatic biological communities (Nicklow & Muleta, 2001). As part of a senior thesis at Allegheny College, Seitz (2011) conducted a sediment analysis in various perennial streams and ultimately determined that sediment loading can significantly impact fish index of biotic integrity scores. Satellite-based data was utilized to examine land cover as part of the overall analysis.

Other studies have made use of land cover data while investigating nutrient loading and eutrophication. Ostrofsky and Bradley (2006) studied phosphorus loading to determine the degree of eutrophication in Northwestern Pennsylvania lakes. The objective of this study was to estimate historical concentrations of phosphorus to compare them to current levels in these lakes. Ultimately, it was predicted that six of the seven lakes studied were mesotrophic before European settlement, meaning that they contained moderate levels of phosphorus even before significant human alteration of the landscape (Ostrofsky & Bradley, 2006). This was accomplished through the creation of a watershed model using land cover (Ostrofsky & Bradley, 2006). This study examined the land cover within entire watersheds as well as within differently sized riparian buffers (Ostrofsky & Bradley, 2006).

The primary studies of interest here were conducted by aquatic ecologists Mark Kirk and Scott Wissinger along with Allegheny College students. The primary focus of this research is to evaluate stream health and create an index of biotic integrity as part of the Pennsylvania Fish and Boat Commission's Unassessed Waters Initiative (Kirk & Wissinger, 2019). More recently, Mark Kirk's research has emphasized the identification and prioritization of streams for the reintroduction of brook trout (*Salvelinus fontinalis*). The brook trout is a vital indicator species for stream habitats as it is very sensitive to changes in its habitat (Taylor, n.d.). It is native to much of eastern North America, but is becoming increasingly confined to remote streams at higher elevations (Taylor, n.d.). Brook trout populations have been severely reduced or extirpated in many watersheds as a result of changes in water quality and land

use practices, increasing water temperature, invasive species, habitat fragmentation, habitat degradation, and habitat destruction (Hudy et al., 2008; Marschall & Crowder, 1996). According to one study, forest cover loss was the primary factor in stream degradation (Stranko et al., 2008). Brook trout presence is dependent on three main factors: the macroinvertebrate and fish communities in streams, water chemistry and temperature, and landscape variables, such as the size of the watershed, the gradient of the stream, and land cover composition (Hudy et al., 2008; Kirk et al., 2017). Stranko et al. (2008) determined that the presence of forested land cover was the strongest predictor of brook trout occurrence. Additionally, with the exception of one stream, no brook trout were found in streams whose watersheds contained over 4% impervious land cover (Stranko et al., 2008). DeWeber and Wagner (2014) determined that brook trout were less likely to occur in streams surrounded by agriculture or developed land cover. However, overall land cover composition may not be as important as long as a 30-meter riparian buffer around a stream is forested (Kirk & Wissinger, 2020). Land cover in a watershed can be composed of 80% agricultural land and still support brook trout if the riparian zone remains intact (Kirk & Wissinger, 2020). Clearly land cover is an extremely important factor for brook trout reintroduction. As a result, it is vital that the land cover data being utilized is as accurate as possible.

All of the aforementioned studies have utilized land cover data from the National Land Cover Database (NLCD). The NLCD is generated using Landsat satellite imagery and special algorithms. It is produced by the Multi-Resolution Land Characteristics (MRLC) Consortium, a cooperative of federal agencies that provide land cover data for all 50 states as well as Puerto Rico (*Multi-Resolution land characteristics (MRLC) Consortium*, n.d.). This data is readily available for public use and provides land cover information about any location within the United States dating back to 1992. Land cover data from the NLCD has a spatial resolution of 30 meters. Each 30 by 30-meter pixel receives the classification of the predominant land cover type within it. This means that a region could be classified as forest, but still feature a lot of agricultural or developed land. As a result, in detailed large-scale analysis, satellite-based land cover may be over- or underestimating the composition of the site (Cleve et al., 2008). The NLCD was utilized in the previously mentioned studies due to a lack of time and resources, the large number of study sites, and a lack of student expertise in GIS. Kirk and Wissinger's work over the past 15 years has involved over 300 sites, with a large amount of the work being conducted in a class environment or as part of senior thesis projects (C. Shaffer, personal communication, March 29, 2022). Obtaining land cover for the watersheds has usually been a very small part of these projects, with a much larger emphasis being placed on field work (C. Shaffer, personal communication, March 29, 2022). Due to the coarse resolution of the NLCD, it is possible that there was a lack of detailed land cover information for the 30-meter riparian buffers examined by Kirk and Wissinger. Since the NLCD has a resolution of 30 meters, the riparian zones for each stream may have been represented by only one or two rows of pixels. Although

manual classification of aerial photography could present a more accurate alternative due to the resolution of the aerial photos, this method would have been too time consuming and tedious.

This study examined the impact of spatial resolution on the accuracy of land cover mapping at the large watershed scale and the possibility of automating the process of image classification as a potential alternative to using the NLCD. This was accomplished by comparing coarse resolution NLCD satellite data and high-resolution air photo image classification data generated through the conversion of raw spectral data to thematic data. Percentages of each land cover type were estimated for both the NLCD and the classified image for each site. Overlay analysis was also performed in order to identify common misclassifications. Overall watershed and riparian zone land cover were examined separately. This study produced fine resolution land cover data as well as an image classification model that can be reused in future studies. A secondary goal was to make a recommendation for or against this method based on the accuracy, ease of use, and efficiency of the image classification process.

## Methods

### Study Region

ArcGIS Pro and the Image Analyst extension (version 2.8.1, ESRI, 2022) were used to generate and compare fine resolution land cover data obtained from multispectral aerial photography and coarse resolution NLCD satellite imagery.

French Creek originates in Chautauqua County, New York and flows southward through Erie, Crawford, Mercer, and Venango Counties in Pennsylvania until it joins the Allegheny River near Franklin, Pennsylvania (French Creek Valley Conservancy, 2019). The main branch of French Creek is approximately 117 miles long and the watershed has an area of about 1,250 square miles or 800,000 acres (French Creek Valley Conservancy, 2019). The watershed is located almost entirely within the Northwestern Glaciated Plateau, with elevations ranging from 1,000 to 1,900 feet (Western Pennsylvania Conservancy, n.d.). The basin is notable for a variety of reasons including its unique geological history, high water quality, and high aquatic diversity (French Creek Valley Conservancy, 2019; Kirk & Wissinger, 2020). French Creek has the highest number of fish species of conservation concern in Pennsylvania (Kirk & Wissinger, 2020). The watershed is comprised primarily of forested land, with deciduous forest accounting for 41.7% of the land (McMillen, n.d.). Agriculture is another dominant land cover class, with 4.5% of the land in the watershed being used for cultivated crops and 34% being used as open pasture (Kirk & Wissinger, 2020; McMillen, n.d.).

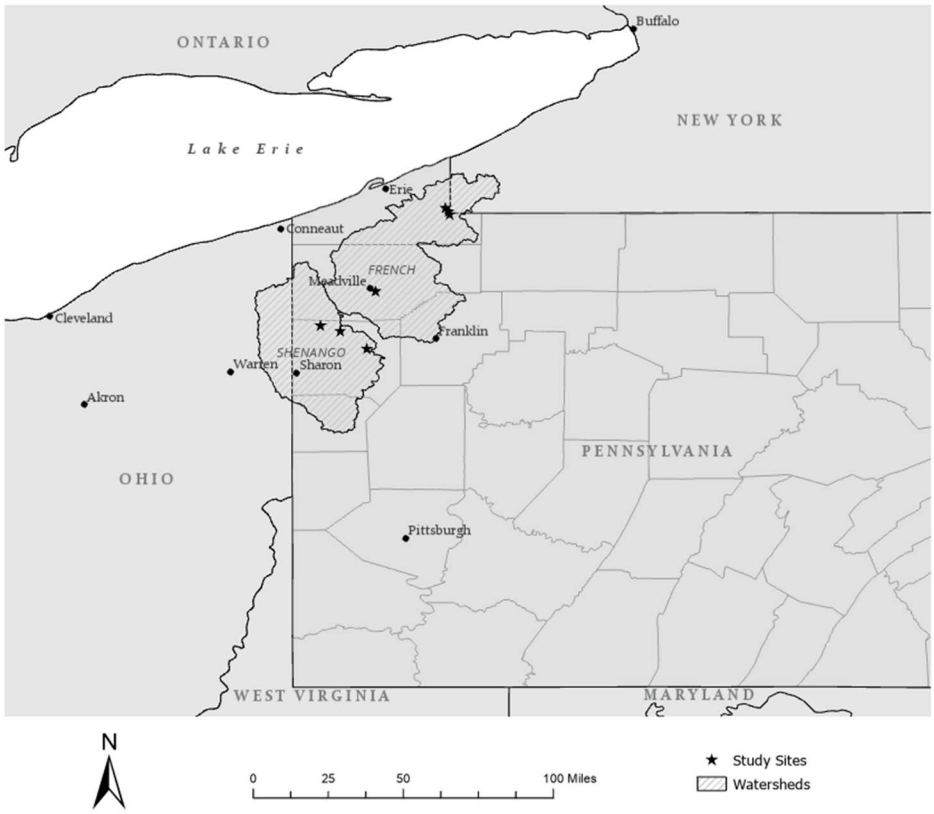



**Figure 1.** Location of study sites within the French Creek and Shenango River watersheds in northwestern Pennsylvania.

The Shenango River originates in Crawford County, Pennsylvania and flows south from Pymatuning Lake, the largest man-made reservoir in the state ("Watersheds," 2015). Once it reaches a point near New Castle in Lawrence County, it joins with the Mahoning River to form the Beaver River, which later empties into the Ohio River ("Watersheds," 2015). Shenango River is approximately 92 miles long and has various tributaries within Crawford County, including Paden Creek, Linesville Creek, and Crooked Creek ("Watersheds," 2015). The basin has an area of 1066 square miles or 680,000 acres; 781 of these square miles are within the state of Pennsylvania ("Watersheds," 2015; Western Pennsylvania Conservancy, 2005). The entire watershed falls within the Appalachian Plateau province. Elevations range from 760 feet to 2200 feet, varying a great deal in different subsections of the province (Western Pennsylvania Conservancy, 2005). The primary land cover in the watershed is agriculture at 46%, but this is closely followed by forested land at 40% (Western Pennsylvania Conservancy, 2005). Like French Creek, the Shenango River watershed is one of the most diverse watersheds in Pennsylvania, primarily due to the presence of wetlands (Western Pennsylvania Conservancy, 2005). Over 30 mammal species

and 60 bird species reside within the watershed year-round, and the river is known for its aquatic diversity ("Watersheds," 2015; Western Pennsylvania Conservancy, 2005).

As part of their studies on stream health and brook trout, Mark Kirk and Scott Wissinger have created indices of biotic integrity for many small watersheds within the French Creek and Shenango River watersheds. For this study, a subset of 6 of these small streams were selected. Streams were selected with the intention of capturing a variety of land cover types both within the watersheds and in the riparian zones surrounding the streams. In order to test the image classification methodology on a primarily urban watershed, Mill Run watershed in the city of Meadville was also utilized. Watersheds were between 0.2 and 20 square kilometers in size.

**Data Sources**

Land cover data was obtained from NLCD 2019, which was generated using Landsat Analysis Ready Data (ARD). The NLCD is released on a two-to-three-year cycle and has a spatial resolution of 30 meters (*Multi-Resolution land characteristics (MRLC) Consortium*, n.d.).

Digital aerial photographs taken in 2019 were obtained from the National Agriculture Imagery Program (NAIP). NAIP imagery is generated with the primary purpose of maintaining Common Land Unit boundaries and assisting with farm programs (USDA, 2015). These photographs are acquired on a two-year cycle during peak growing season (USDA, 2015). Most NAIP Imagery is acquired using digital sensors at a one-meter ground sample distance (USDA, 2015). More recently, 0.6-meter ground sample distance imagery has been offered, providing extremely fine resolution data. This fine spatial resolution provides much more detail than the NLCD, which in theory, could facilitate more detailed land cover data. Each image tile has four bands (red, green, blue, and near-infrared). Color-infrared imagery was utilized during image classification in order to aid in the process of interpretation. Vegetation primarily absorbs red and blue light to be used as energy for photosynthesis (John Innes Centre, 2021; Knipling, 1970). Green light is not required for this process, so more of this is reflected, leading the human eye to perceive plants as the color green (John Innes Centre, 2021; Knipling, 1970). However, peak reflectance actually occurs in the near-infrared range (Knipling, 1970). Color-infrared imagery using the red, green, and infrared bands is created by assigning the infrared band to the red channel. For this reason, vegetation appears in various shades of red or pink in color-infrared imagery (Weng, 2021, p. 205). The hue varies based on the type and health of the vegetation (Weng, 2021, p. 205). It was vital to work with aerial photographs from the same year that the NLCD datasets were generated in order to make an accurate comparison. The NAIP imagery utilized had a spatial resolution of 0.6 meters.

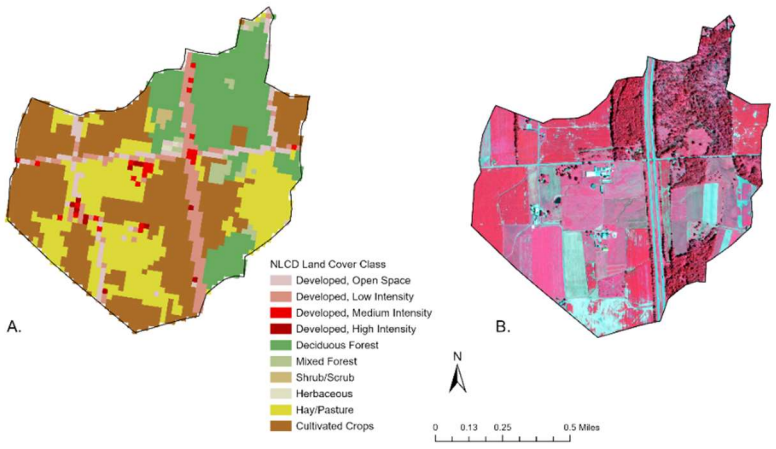



**Figure 2.** Data Sources. (A) Land cover data obtained from the NLCD. This data was clipped to the watershed for study site MAK 331. (B) Aerial photograph obtained from the NAIP displayed using near-infrared, red, and green bands.

**Data Manipulation**

Before image classification could occur, the data needed to be standardized in order to perform overlay analysis. All of the data was projected to NAD 1983 UTM Zone 17N. Larger datasets were subsetted to the region of geographic interest. Areas larger than the watershed were processed in order to ensure sufficient training samples could be created.

**Data Analysis**

There are two major approaches to image classification: unsupervised classification and supervised classification (Weng, 2012, p. 207). In unsupervised classification, images are classified into categories by their digital numbers without the use of training samples (Olaode et al., 2014). This relies on machine learning algorithms and does not require any human intervention (Nath et al., 2014; Olaode et al., 2014). ISODATA (Iterative Self-Organizing Data Analysis Technique) is the most common method. This technique involves the use of a maximum-likelihood decision rule, which "calculates class means that are evenly distributed in the data space" (Melesse & Jordan, 2002). The remaining pixels are classified with minimum distance techniques (Melesse & Jordan, 2002). This process repeats multiple times until a certain threshold is met (Melesse & Jordan, 2002). Later, the groups created by the computer can be combined or broken down manually if necessary (Weng, 2012, p. 208).

Supervised classification involves the use of training areas, which are representative samples of each cover type or information class (Weng, 2012, p. 208). The spectral signature of each class is based on the digital numbers of the pixels in the training areas (Weng, 2012, p. 208). These signatures are then

used to classify all of the pixels in an image into informational classes (Nath et al., 2014). It is vital to provide between 30 and 50 training samples for each class to ensure accurate classification (Liedtke & Hu, 2018; Lu & Weng, 2007). Supervised classification can be labor-intensive and time consuming, but it generally has higher accuracy than unsupervised classification since an operator can detect and rectify errors (Nath et al., 2014). This study utilized supervised classification.

**Table 1.** Advantages and Disadvantages of supervised and unsupervised classification. In a paper comparing the accuracy of supervised and unsupervised classifications, Enderle & Weih (2005) provided a variety of advantages and disadvantages to both methods.

| Classification Type | Advantages | Disadvantages |
|---|---|---|
| Unsupervised Classification | No extensive knowledge of region required<br>Opportunities for human error are minimized<br>Can be used to create or evaluate training samples<br>Unique classes are recognized | Classes are spectrally homogenous, may not correspond with informational classes<br><br>Analyst has limited control over classes |
| Supervised Classification | Total control of classes or informational categories<br>Classes are tailored to specific sites<br>Analyst doesn't have to match spectral classes to informational classes<br>Can compare training samples to final data in order to detect serious errors | Defined based on informational categories rather than actual spectral signature<br><br>Careful selection is time and labor intensive, requires extensive knowledge<br>Training sites may not represent unique classes |

A variety of different classifiers can be used when carrying out supervised classification. A classifier is defined as a "computer program that implements a classification procedure" (Weng, 2012, p. 209). There are pixel-based classifiers, where individual pixels are classified, and object-based classifiers, where groups of neighboring pixels with similar spectral signatures are segmented into objects and these objects

are classified (Morgan et al., 2010). Object-based methods of image classification tend to be more accurate than pixel-based classifiers and are now considered the standard classification method (Liu & Xia, 2010; Ma et al., 2017). This is partially because using objects instead of pixels helps to reduce spectral variation within classes (Liu & Xia, 2010). Additionally, it has been demonstrated in multiple studies that pixel-based classifiers do not perform as well with high-spatial-resolution images due to the increase in spectral variability in finer resolution images (Guo et al., 2007). Cleve et al. (2008) conducted both a pixel-based and object-based analysis of urban land cover and found that the object-based method was 41.73% more accurate for the built-area category. Using an object-based classifier also generally eliminates the issue of salt-and-pepper effects (Kelly et al., 2011; Liu & Xia, 2010). Salt-and-pepper effects are a type of noise that occur when there is "high local spatial heterogeneity between neighboring pixels" (Kelly et al., 2011). This can result in individual pixels inaccurately receiving a different classification than surrounding pixels. For these reasons, object-based classification was used in this study.

The primary distinction between the object-based classification workflow and pixel-based methods is segmentation, in which neighboring pixels with similar spectral signatures and shapes are grouped together. These objects are then classified rather than individual pixels. The default values for each of the three parameters in software were used, meaning that spectral detail was set to 15.50, spatial detail was set to 15, and minimum segment size in pixels was set to 20.

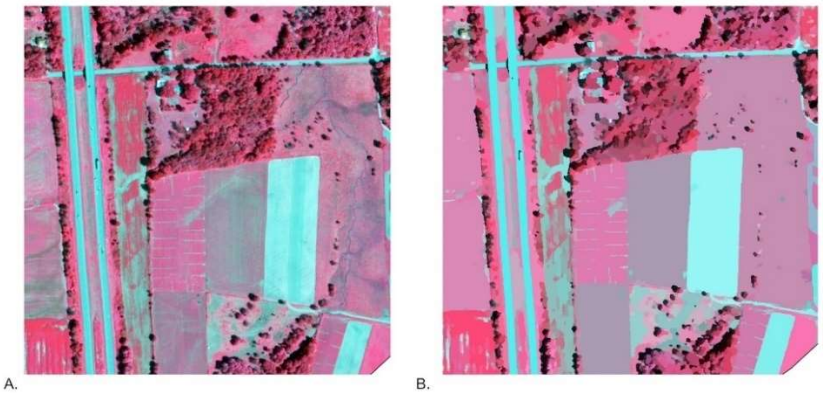



**Figure 3.** Segmentation Results. (A) Aerial photograph obtained from the National Agriculture Imagery Program (NAIP) prior to segmentation. (B) Aerial photograph following segmentation.

Training areas were created in order to develop a spectral signature for each land cover type. When possible, training sites were generated using the results of the segmentation. When segments included multiple land cover types, training sites were digitized manually.

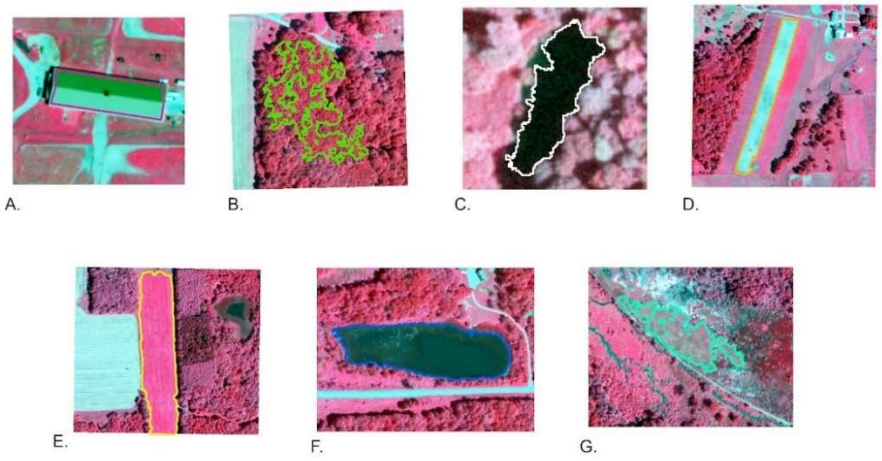



**Figure 4.** Example Training Samples. Training samples were created for each land cover type as part of the supervised classification workflow. (A) Developed, (B) Forested, (C) Shadow, (D) Tilled agriculture, (E) Vegetated agriculture, (F) Water, (G) Wetlands.

There are a variety of classifiers that can be used for object-based classification. A meta-analysis comparing the utility of many of these different supervised learning methods for land cover image classification determined that the Random Forest/Trees classifier was the most accurate, followed by the Support Vector Machine (SVM) classifier (Ma et al., 2017). The Random Trees classifier was utilized in this study; default parameters were used. After image classification occurred, some manual reclassification was conducted in order to improve the accuracy of the classified image. Polygons are drawn around misclassified areas. Pixels within this polygon receive a new classification. Only areas within watershed boundaries were reclassified.

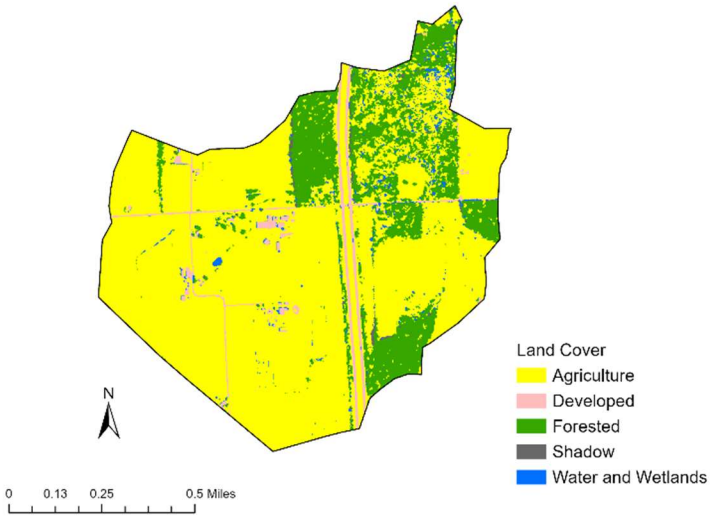



**Figure 5.** Image Classification Results. Aerial photograph obtained from the NAIP classified using object-based classification in the watershed for study site MAK 331. The Random Trees classifier was utilized.

For this study, the land cover classes identified in Mark Kirk's brook trout studies were used. These include natural cover, agricultural areas, and developed areas (Kirk et al., 2017; Kirk & Wissinger, 2019). The results of the image classifications and the NLCD data were reclassified into these three categories. For the classified aerial photographs, the water and wetlands and forested classes were merged into the category of natural cover. For the NLCD images, the four developed land cover classes were reclassified as developed, hay/pasture and cultivated crops were merged into the category of agriculture, and deciduous forest, mixed forest, herbaceous, and shrub/scrub were all reclassified as natural cover.

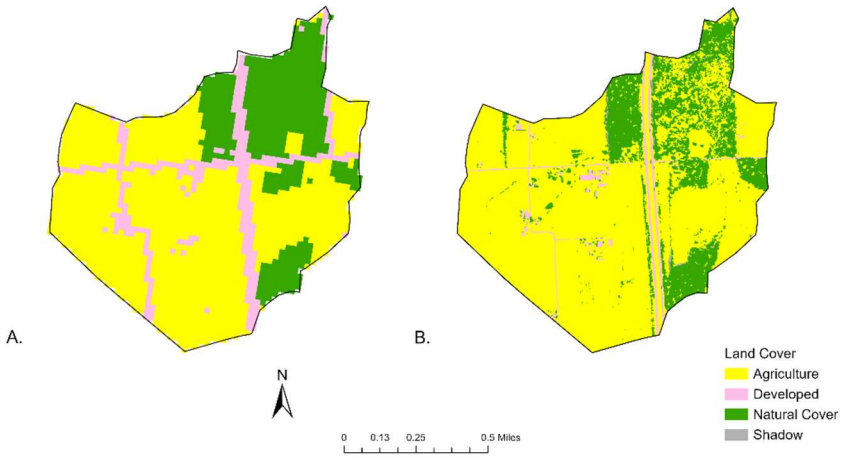



**Figure 6.** Reclassified Land Cover Data. (A) Land cover data obtained from the National Land Cover Database (NLCD) reclassified into natural cover, agriculture, and developed. (B) Land cover data generated through object-based image classification reclassified into natural cover, agriculture, developed, and shadow.

An error matrix was utilized to evaluate the accuracy of the image classifications. For each site, 75 points were randomly generated and these locations on the classified image were visually compared to the original aerial photograph. The last step was to compare the classified image data to the NLCD land cover data. The percentage of pixels in each land cover class was calculated for each watershed and each 30-meter riparian buffer. The differences between the percentage of each land cover type in the classified image and the reclassified NLCD data were calculated.

**Table 2.** Sample Error Matrix. Classification values correspond to different land cover classes. Values of 1 indicate that a point received an accurate classification; values of 0 indicate a misclassification.

| ID | Classified | Ground Truth |
|---|---|---|
| 1 | 3 | 1 |
| 2 | 1 | 0 |
| 3 | 4 | 0 |
| 4 | 2 | 1 |
| 5 | 1 | 1 |

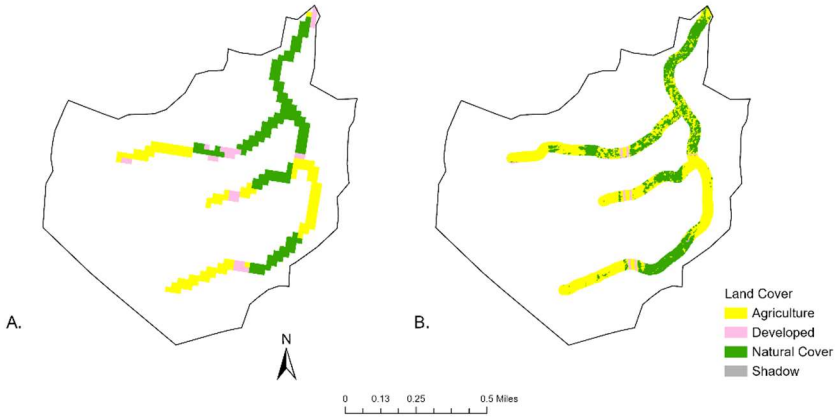



**Figure 7.** Land Cover in the Riparian Buffer. (A) Land cover data obtained from the NLCD clipped down to 30-meter riparian buffer. (B) Land cover data generated through object-based image classification clipped down to 30-meter riparian buffer.

Overlay analysis was also utilized to compare the reclassified NLCD and the classified NAIP images. The NLCD was resampled to a spatial resolution of 0.6 meters to match the NAIP imagery. Areas that received different classifications between the two datasets were identified by combining the two layers. These areas were then analyzed under the assumption that the classified image was more accurate. The goal of this overlay was to determine what misclassifications were most likely to occur in the NLCD and where. Percentages were calculated in order to determine how much the NLCD differed from the classified image for each of the three land cover classes. Misclassified areas were then examined to determine which misclassifications were most likely to occur. For example, if an area is classified as developed in the NLCD, but received a different classification in the image classification process, that would mean it was either natural cover or agriculture. Of the pixels that were misclassified as developed, the percentages of pixels that should have been classified as natural cover or agriculture were calculated. This was done for all three land cover classes at each site. These values were then averaged.

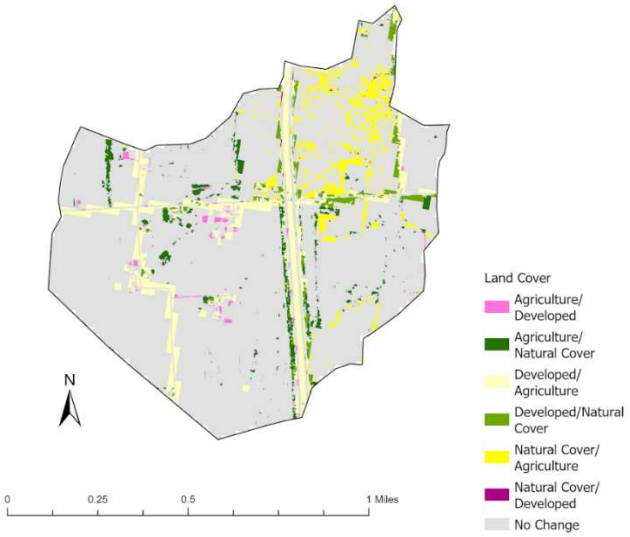



**Figure 8.** Overlay Analysis Comparing NLCD and Classified Image. Colored areas represent places in which the classification differed between the NLCD and the classified image. The first word in the legend indicates the classification that an area received in the NLCD while the second word is the classification that this area received through the process of image classification.

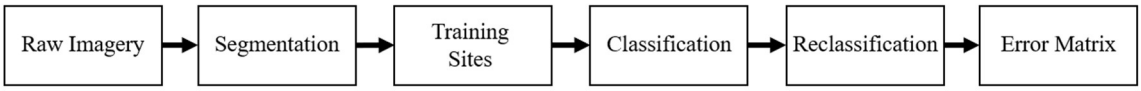



**Figure 9.** Image Classification Flowchart.

## Results

Classifications resulted in 96.6% accuracy on average (Table 3). The standard minimum accuracy for remotely sensed land cover image classification is 85% (Manandhar et al., 2009). Each site had a level of accuracy that exceeded this value (Table 3).

**Table 3.** Error Matrix Results. Accuracy of image classification for each site determined using error matrices.

| Site | Accuracy (%) |
|---|---|
| MAK 320 | 100.0 |
| MAK 321 | 97.3 |
| MAK 331 | 100.0 |
| MAK 355 | 93.3 |
| MAK 375 | 98.7 |
| MAK 386 | 94.7 |
| Mill Run | 92.0 |
| Average | 96.6 |

Following reclassification, the percentage of each land cover type was calculated for both the classified aerial photograph and the NLCD data for each site. This was done for both entire watersheds and the 30-meter riparian buffer around each stream. The differences between these percentages were calculated and averaged (Table 4, Table 5).

On average, the most significant difference between the NLCD and the classified image occurred in the developed category. The differences between the percentage of developed land varied from site to site, with the Mill Run site indicating a -25% difference and site MAK 355 indicating only a -0.9% difference. The difference for all of the developed sites was a negative number, meaning that the NLCD had a higher percentage in each site. The average differences between the percentages of agriculture and natural cover were less significant, but some individual sites had major differences. Site MAK 331 had a difference of 8.7% in the agriculture category while Mill Run had a difference of 13.5% in the agriculture category. Site MAK 321 demonstrated the largest difference in the percentage of natural cover at 5.1%.

**Table 4.** Average Difference Between NLCD and Classified Image. Positive values indicate that the NLCD had less of this land cover type when compared the classified image, while negative values indicate that the NLCD had more of this land cover type.

| Land Cover Class | Agriculture (%) | Developed (%) | Natural Cover (%) |
|---|---|---|---|
| Average Difference | 4.2 | -8.7 | 1.0 |
| Standard Deviation | 5.8 | 8.4 | 3.1 |

The most significant difference between the NLCD and the classified image within the riparian zone also occurred in the developed category. The largest difference occurred in the Mill Run riparian zone at -19.3%. There was no difference at site MAK 355 as there was no developed land cover within the riparian zone at this site. The smallest difference excluding this site was the -2.0% difference at site MAK 321. The average differences between the percentages of natural and agricultural land cover were very small, but with some significant deviation. Natural cover differed by 8.1% in the riparian zone at site MAK 355 and agricultural land cover differed by -11.0%. Agricultural land cover in the riparian zone differed by 13.2% at Mill Run and 9.4% at MAK 331.

**Table 5.** Average Difference Between NLCD and Classified Image for 30-meter Riparian Buffer. Positive values indicate that the NLCD had less of this land cover type when compared the classified image, while negative values indicate that the NLCD had more of this land cover type.

| Land Cover Class | Agriculture (%) | Developed (%) | Natural Cover (%) |
|---|---|---|---|
| Average Difference | 1.7 | -5.7 | -0.1 |
| Standard Deviation | 8.4 | 6.4 | 5.5 |

NLCD accuracy in comparison to the classified images was determined for each land cover class. Assuming that the classified images are 100% accurate, NLCD accuracy could be estimated by finding the percentages of pixels that were the same or differed between the two datasets. On average, 83.7% of the pixels in the agriculture class and 87.4% of the pixels in the natural cover class were the same in the NLCD and the classified image (Table 5). Only an average of 14.5% of the pixels classified as agriculture in the NLCD received the same classification in the classified NAIP image, with 80% receiving a different classification (Table 5).

**Table 6.** NLCD Accuracy by Land Cover Category. Percentages were calculated to determine how much the NLCD differed from the classified NAIP image for each of the land cover classes. Percentages do not add up to 100 because areas classified as shadow were disregarded.

| Site | Agriculture No Change | Agriculture Change | Developed No Change | Developed Change | Natural Cover No Change | Natural Cover Change |
|---|---|---|---|---|---|---|
| MAK 320 | 90.7% | 8.0% | 15.3% | 82.3% | 91.8% | 6.0% |
| MAK 321 | 75.1% | 23.9% | 13.2% | 80.5% | 96.2% | 2.6% |
| MAK 331 | 94.7% | 4.6% | 23.2% | 73.7% | 76.8% | 19.3% |
| MAK 355 | 93.3% | 6.2% | 6.0% | 93.9% | 93.6% | 4.2% |
| MAK 375 | 82.2% | 14.4% | 11.5% | 82.6% | 89.9% | 6.7% |
| MAK 386 | 77.9% | 19.7% | 8.1% | 86.7% | 86.5% | 10.3% |
| Mill Run | 72.1% | 19.0% | 24.4% | 60.1% | 76.9% | 14.1% |
| Average | 83.7% | 13.7% | 14.5% | 80.0% | 87.4% | 9.0% |
| STDEV | 9.2 | 7.5 | 7.1 | 10.7 | 7.8 | 5.9 |

Following this analysis, only misclassified pixels were examined. Areas of natural cover and agriculture were more likely to be mistaken for one another than for developed land. Most areas that were wrongfully classified as developed were actually agricultural or vegetated land. The areas that were reported as developed in the NLCD and not in the classified images are visible in the figures generated

through overlay analysis (Fig. 8, 12, 15, 18, 21, 24). The excess developed area around each road is one of the most noteworthy aspects of the overlays. Another aspect of these figures that stands out is the sharp edges of the much larger NLCD pixels (Fig. 8).

**Table 7.** Misclassified Pixels and their Corresponding Real World Cover Types. Percentages represent which classes were more likely to be misclassified in the NLCD as a certain class.

| NLCD Developed | | NLCD Agriculture | | NLCD Natural Cover | |
|---|---|---|---|---|---|
| Agriculture | Natural Cover | Developed | Natural Cover | Agriculture | Developed |
| 64.5% | 35.5% | 5.9% | 94.1% | 98.6% | 1.4% |

## Discussion

This study was conducted in order to evaluate the difference between land cover obtained from the NLCD and land cover generated through image classification of NAIP aerial photography, determine where potential misclassifications occur, and assess which method is a more accurate and efficient option for Mark Kirk's future brook trout studies. Since the NLCD has a relatively coarse spatial resolution of 30 meters, it is possible that certain land cover classes are being over- or underestimated. Supervised, object-based image classification of fine resolution aerial photography could provide more accurate land cover information with only some additional effort.

Following manual reclassification, all classifications surpassed the 85% minimum accuracy standard (Manandhar et al., 2009). With an average accuracy of 96.6%, it would appear that supervised, object-based image classification is a viable option for the creation of land cover imagery for watersheds smaller than 20 square kilometers. After comparing these classifications to the NLCD, it became clear that the NLCD has a tendency to overestimate the amount of developed land. Due to the coarse resolution of the NLCD, vegetated land very close to roads, large buildings, and groups of houses was often misclassified as developed. Unexpectedly, more significant differences were seen in the percentages of each land cover type within entire watersheds than within riparian zones. However, the average differences within the riparian zones have a larger standard deviation. It is possible that individual sites could see larger differences in the riparian zone. Overlay analysis further highlighted the overestimation of developed land. Only 14.5% of the pixels classified as developed in the NLCD received the same classification in the classified images, with 80% receiving a different classification (Table 5). The figures generated through this analysis illustrate the ways that roads or buildings can be generalized by the NLCD. A typical lane on a state road in the United States is about 12 feet or 3.7 meters wide. If a pixel in

the NLCD contains at least 50% developed land, then a road can be stretched out to 30 meters. In areas with a lot of buildings or impervious surfaces, yards and other small areas of vegetation are lost. Many differences between the NLCD and classified image appear to occur at boundaries between land cover types. The edge of a forest or agricultural field may be misclassified due to the spatial resolution of the NLCD. Small areas of trees within agricultural fields were often missed as well. Overlay analysis demonstrated that areas inaccurately classified as developed should have been classified as agriculture almost two-thirds of the time. On the other hand, areas misclassified as agriculture were almost always actually natural cover and vice-versa. Image classification clearly has the potential to provide land cover data with increased accuracy, especially with regard to impervious surfaces, but the process can be time-consuming and labor-intensive. This methodology is probably best suited to projects using broad land cover categories and a relatively small number of sites. For example, Seitz (2011) studied 8 streams and utilized only 4 land cover categories in their sediment analysis: natural cover, developed, pasture and hay, and row crops. This study could benefit greatly from the increased accuracy of land cover derived through image classification. On the other hand, Ostrofsky and Bradley (2006) utilized 13 different land cover classes in their study on eutrophication and phosphorous loading, several of which would be difficult to distinguish with this method. Examples include woody wetlands, emergent herbaceous wetlands, deciduous, evergreen, and mixed forest, as well as various levels of development. Mark Kirk's ongoing stream health and brook trout research uses three broad land cover categories and generally involves about 10-15 study sites per year. Additionally, forested land cover is the strongest predictor of brook trout occurrence, making it very important for any studies focused on them to have accurate data (Stranko et al., 2008). Although image classification of NAIP imagery requires more effort than utilizing the NLCD, the increased accuracy could potentially influence Mark Kirk's research on brook trout reintroduction.

The methods utilized in this study are supported by a variety of research. Rwanga and Ndambuki (2017) classified Landsat imagery using pixel-based supervised classification in order to create land cover data. Land cover categories included agriculture, water body, built up areas, mixed forest, shrubs, and barren/bare land (Rwanga & Ndambuki, 2017). Error matrices and statistical analysis were utilized to evaluate classification accuracy (Rwanga & Ndambuki, 2017). Their classification resulted in 81.7% accuracy (Rwanga & Ndambuki, 2017). Rodriguez-Galiano et al. (2012) utilized the Random Forest classifier for land cover classification of Landsat imagery. The kappa statistic was used to determine that their classification was 92% accurate. Ma et al. (2017) conducted a meta-analysis in which the results of various studies using object-based land cover classification were reviewed. Ultimately, Ma et al. (2017) determined that Random Forest was the most accurate classifier for this application, followed closely by SVM. Other trends were also evaluated. Classification accuracy became higher with higher resolution images (Ma et al., 2017). Powers et al. (2012), one of the studies examined by Ma et al. (2017), resampled

images to various spatial resolutions and performed object-based classification. Wetland classification accuracy was highest when a spatial resolution of 10 meters was used (Powers et al., 2012). Each classification was evaluated individually using sample points; these classifications were then compared using scale-based change detection methods (Powers et al., 2012). Object-based classification was almost always used on fairly small areas, with 95.6% of the studies examined by Ma et al. (2017) focusing on a region smaller than 300 hectares. The majority of the studies analyzed used high resolution data obtained from satellites or unmanned aerial vehicles (UAV) (Ma et al., 2017). There was also a trend of higher accuracy for more homogeneous areas or land cover types (Ma et al., 2017). For example, complex urban landscapes were more difficult to classify than agricultural land (Ma et al., 2017).

Li and Shao (2014) used object-based land cover classification methods on NAIP imagery for Tippecanoe County in Indiana. This study compared the accuracy of this method to pixel-based methods, with the pixel-based maximum likelihood method resulting in 79% accuracy while the object-based method achieved 93% accuracy (Li & Shao, 2014). Although they did not compare their results to NLCD as part of their study, Li and Shao (2014) discussed its limited accuracy due to its relatively coarse resolution in comparison to the very high resolution NAIP imagery. Specific examples of errors were provided, including a small, forested area that was classified as woody wetlands, a lack of distinction between roads and buildings in some residential areas, and inaccurately shaped crop fields (Li & Shao, 2014). They also determined that pixels in the NLCD containing multiple land cover types or with similar spectral responses are more likely to be misclassified (Li & Shao, 2014).

Although this methodology was successful in creating land cover divided into the categories of agriculture, developed, and natural cover, it is unclear if this method would be suitable if more categories were desired. For example, wetland classification is notoriously difficult from a remote sensing perspective (Mahdavi et al., 2017). Different wetland types are similar ecologically and spectrally both to one another and to other land cover classes (Mahdavi et al., 2017). Additionally, wetlands usually don't have sharply defined borders, but rather transition into other land cover types (Mahdavi et al., 2017). The presence of water can be helpful in identifying wetlands, but this is not always useful as it can be underground or vary significantly from season to season (Mahdavi et al., 2017). Because of all of these factors, it is difficult for both the software and the analyst to identify wetlands. Another limitation relates to the NLCD's developed, open space land cover class. Developed, open space is officially defined as "areas with a mixture of some constructed materials, but mostly vegetation in the form of lawn grasses, and impervious surfaces accounting for less than 20% of total cover" (Esri, 2021). In this study, only impervious surfaces were treated as developed land cover. Areas that would be considered developed, open space by the NLCD were classified as agriculture due to their similar spectral signatures. It is possible that this has resulted in an underestimation of developed land cover and an overestimation of

agricultural land. This may have contributed to why almost two-thirds of the pixels that were identified as developed by the NLCD, but were placed in a different category during the image classification process, were classified as agriculture.

Another limitation is that the overlay analysis for this study was conducted with the assumption that the results of image classification were completely accurate, which was not the case. Although an average accuracy of 96.6% was achieved, this value was derived entirely from error matrices. Unlike Rwanga and Ndambuki (2017) and Rodriguez-Galiano et al. (2012), this study did not verify accuracy using sensitivity analysis or methods of statistical analysis like Cohen's kappa. Additional analysis would be necessary in order to truly determine classification accuracy. This factor does not invalidate the overlay analysis that was performed, but it is an important consideration to keep in mind when interpreting the results.

Larger sites with more variety seemed to have more errors in the classification process. This observation is supported by Ma et al.'s (2017) finding that more homogeneous areas tend to have higher classification accuracy. Mill Run was the most challenging watershed to classify by far, due to its size and variety. Additionally, in the year 2019, when all of the remotely sensed data was collected, a major lake within Mill Run was drained. It is possible that this led to decreased classification accuracy. Many areas were mistakenly classified as wetlands as a result. Other limitations included confusion between water and shadows. Although an analyst can easily distinguish between these classes, the software had some difficulty as they are spectrally similar. It is possible that this confusion increased the percentage of pixels classified as natural cover. Land cover percentages were also influenced by the fact that the methodology utilized does not include manually reclassifying areas covered in shadow to what is actually underneath. For that reason, areas in shadow were missed entirely.

Although the default parameters provided the best segmentation results, these results were still not ideal. Forested areas were over-segmented, leading to a problem where image classification would produce results in which agriculture and wetlands were speckled through the forest. When parameters were changed to combat this problem, accuracy was reduced elsewhere due to under-segmentation. Many buildings became deformed, and the software could not differentiate between agriculture and forest in several areas. Including manual reclassification in this study allowed for increased accuracy but reduced the efficiency of the overall process. Additionally, unexplainable glitches were encountered that prevented some reclassifications from being implemented. The source of these errors was unable to be determined. These unresolvable errors reduced classification accuracy to a certain degree.

An interesting possibility for future research would be an in-depth examination of whether or not wetlands can be accurately classified through supervised, object-based classification. Wetland classification with remote sensing techniques is challenging, but extremely valuable as it reduces the need

for field work (Mahdavi et al., 2017). Several studies have reported increased accuracy in wetland classification through the use of imagery captured using polarized synthetic aperture radar or SAR (Mahdavi et al., 2017). SAR is a form of active remote sensing in which a sensor that is installed on a moving platform transmits electromagnetic pulses and records the light that is reflected back (Moreira et al., 2013). Mahdavi et al. (2017) reported that HH polarization is most effective in delineating wetlands. Another strategy could involve comparing the results of wetland classification to data from the National Wetland Inventory or the NLCD. If successful wetland classification is achieved, this method could be used for applications that include wetlands as an individual category. Another recommendation for future research would be to conduct a similar analysis, but with the addition of a class for developed, open space. It is unclear if the software would successfully be able to distinguish between these areas and vegetated agriculture, but if this could successfully be implemented, classification accuracy would be improved.

This project compared land cover from the NLCD to land cover generated through supervised, object-based classification of aerial photography. These classifications achieved an average accuracy of 96.6%, demonstrating that image classification is a viable method to obtain land cover data for the purposes of this study. The most significant difference between the NLCD and the classified images occurred in the developed class, with larger differences occurring in the watersheds as a whole than in the 30-meter riparian zones. Land cover data generated through image classification may provide increased accuracy, as 80% of developed pixels in the NLCD did not match the classified image. However, limitations related to wetland classification and the existence of the developed, open space category may have influenced these results. Ultimately, whether or not the potential increased accuracy of this method is worth the additional effort is a decision that individual researchers will have to make.

## References


Campbell, J. B., & Wynne, R. H. (2011). *Introduction to remote sensing* (5th ed.). Guilford Press.

Cleve, C., Kelly, M., Kearns, F. R., & Moritz, M. (2008). Classification of the wildland–urban interface: A comparison of pixel- and object-based classifications using high-resolution aerial photography. *Computers, Environment and Urban Systems*, *32*(4), 317–326. https://doi.org/10.1016/j.compenvurbsys.2007.10.001

DeWeber, J. T., & Wagner, T. (2014). Predicting Brook trout occurrence in stream reaches throughout their native range in the eastern United States. Transactions of the American Fisheries Society, 144(1), 11–24. https://doi.org/10.1080/00028487.2014.963256

DiBiase, D. (n.d.). *4. spectral response patterns*. 4. Spectral Response Patterns | The Nature of Geographic Information. Retrieved September 12, 2021, from https://www.e-education.psu.edu/natureofgeoinfo/c8_p5.html.

Enderle, D. I. M., & Weih, R. C. (2005). Integrating Supervised and Unsupervised Classification Methods to Develop a More Accurate Land Cover Classification. *Journal of the Arkansas Academy of Science*, *59*(1), 65–73. Retrieved 2022, from https://scholarworks.uark.edu/cgi/viewcontent.cgi?article=1535&context=jaas.

Esri. (2021, September 8). *USA NLCD Land Cover*. ArcGIS Online. Retrieved April 2, 2022, from https://www.arcgis.com/home/item.html?id=3ccf118ed80748909eb85c6d262b426f

French Creek Valley Conservancy. (2019, August 14). *French Creek Watershed*. French Creek Valley Conservancy. Retrieved December 1, 2021, from https://www.frenchcreekconservancy.org/french-creek-watershed/.

Guo, Q., Kelly, M., Gong, P., & Liu, D. (2007). An object-based classification approach in mapping tree mortality using high spatial resolution imagery. *GIScience & Remote Sensing*, *44*(1), 24–47. https://doi.org/10.2747/1548-1603.44.1.24

Hudy, M., Thieling, T. M., Gillespie, N., & Smith, E. P. (2008). Distribution, status, and land use characteristics of subwatersheds within the native range of brook trout in the Eastern United States. *North American Journal of Fisheries Management*, *28*(4), 1069–1085. https://doi.org/10.1577/m07-017.1

Kelly, M., Blanchard, S. D., Kersten, E., & Koy, K. (2011). Terrestrial remotely sensed imagery in support of Public Health: New Avenues of research using object-based image analysis. *Remote Sensing*, *3*(11), 2321–2345. https://doi.org/10.3390/rs3112321

Khatami, R., Mountrakis, G., & Stehman, S. V. (2016). A meta-analysis of remote sensing research on supervised pixel-based land-cover image classification processes: General guidelines for practitioners and future research. *Remote Sensing of Environment*, *177*, 89–100. https://doi.org/10.1016/j.rse.2016.02.028

Kirk, M. A., & Wissinger, S. A. (2019). Accounting for non-native brown trout in biological assessments: Implications for selecting reference conditions. *Freshwater Science*, *38*(4), 790–801. https://doi.org/10.1086/705918

Kirk, M. A., & Wissinger, S. A. (2020). Assessment of long-term trends in fish distributions at multiple scales decreases uncertainty associated with historical datasets. *Environmental Management*, *66*(1), 136–148. https://doi.org/10.1007/s00267-020-01298-1

Kirk, M. A., Wissinger, S. A., Goeller, B. C., & Rieck, L. O. (2017). Co-varying impacts of land use and non-native brown trout on fish communities in small streams. *Freshwater Biology*, *62*(3), 600–614. https://doi.org/10.1111/fwb.12889

Knipling, E. B. (1970). Physical and physiological basis for the reflectance of visible and near-infrared radiation from vegetation. *Remote Sensing of Environment*, *1*(3), 155–159. https://doi.org/10.1016/S0034-4257(70)80021-9

Li, M., Zang, S., Zhang, B., Li, S., & Wu, C. (2014). A review of remote sensing image classification

techniques: The role of spatio-contextual information. *European Journal of Remote Sensing*, *47*(1), 389–411. https://doi.org/10.5721/eujrs20144723

Li, X., & Shao, G. (2014). Object-based land-cover mapping with high resolution aerial photography at a county scale in Midwestern USA. *Remote Sensing*, *6*(11), 11372–11390. https://doi.org/10.3390/rs61111372

Liedtke, J., & Hu, H. (Producer). (2018). *ArcGIS Pro: Image Segmentation, Classification, and Machine Learning* [Webinar]. https://www.youtube.com/watch?v=v40abIwGZWA

Liu, D., & Xia, F. (2010). Assessing object-based classification: Advantages and limitations. *Remote Sensing Letters*, *1*(4), 187–194. https://doi.org/10.1080/01431161003743173

Loveland, T. R., & Dwyer, J. L. (2012). Landsat: Building a strong future. *Remote Sensing of Environment*, *122*, 22–29. https://doi.org/10.1016/j.rse.2011.09.022

Lu, D., & Weng, Q. (2007). A survey of image classification methods and techniques for improving classification performance. *International Journal of Remote Sensing*, *28*(5), 823–870. https://doi.org/10.1080/01431160600746456

Ma, L., Li, M., Ma, X., Cheng, L., Du, P., & Liu, Y. (2017). A review of supervised object-based land-cover image classification. *ISPRS Journal of Photogrammetry and Remote Sensing*, *130*, 277–293. https://doi.org/10.1016/j.isprsjprs.2017.06.001

Mahdavi, S., Salehi, B., Granger, J., Amani, M., Brisco, B., & Huang, W. (2017). Remote Sensing for wetland classification: A comprehensive review. *GIScience & Remote Sensing*, *55*(5), 623–658. https://doi.org/10.1080/15481603.2017.1419602

Manandhar, R., Odeh, I., & Ancev, T. (2009). Improving the accuracy of land use and land cover classification of landsat data using post-classification enhancement. *Remote Sensing*, *1*(3), 330–344. https://doi.org/10.3390/rs1030330

Marschall, E. A., & Crowder, L. B. (1996). Assessing population responses to multiple anthropogenic effects: A case study with Brook Trout. *Ecological Applications*, *6*(1), 152–167. https://doi.org/10.2307/2269561

McMillen, A. (n.d.). *Land use for French Creek watershed*. French Creek Watershed Research Program. Retrieved March 24, 2022, from http://watershed.allegheny.edu/data/land-use/land-use-for-french-creek-watershed

Melesse, A. M., & Jordan, J. D. (2002). A Comparison of Fuzzy vs. Augmented-ISODATA Classification Algorithms for Cloud-Shadow Discrimination from Landsat Images. *Photogrammetric Engineering & Remote Sensing*, *68*(9), 905–911. Retrieved from https://www.asprs.org/pers-archives-of-the-past?a_tag=2002&a_category=Sep&submit=GO.

Minnesota IT Services. (n.d.). *Land Management Information Center - Minnesota Land Ownership*. Color-Infrared (CIR) Imagery. Retrieved February 25, 2022, from https://www.mngeo.state.mn.us/chouse/airphoto/cir.html

Moreira, A., Prats-Iraola, P., Younis, M., Krieger, G., Hajnsek, I., & Papathanassiou, K. P. (2013). A Tutorial on Synthetic Aperture Radar. *IEEE Geoscience and Remote Sensing Magazine, 1*(1), 6–43. https://doi.org/10.1109/MGRS.2013.2248301

Morgan, J. L., Gergel, S. E., & Coops, N. C. (2010). Aerial Photography: A rapidly evolving tool for ecological management. *BioScience*, *60*(1), 47–59. https://doi.org/10.1525/bio.2010.60.1.9

*Multi-resolution land characteristics (MRLC) consortium*. Multi-Resolution Land Characteristics (MRLC) Consortium. (n.d.). Retrieved February 25, 2022, from https://www.mrlc.gov/

NASA. (2022, February 15). *Data*. NASA Landsat Science. Retrieved February 25, 2022, from https://landsat.gsfc.nasa.gov/data/

Nath, S. S., Mishra, G., Kar, J., Chakraborty, S., & Dey, N. (2014). A survey of image classification

methods and techniques. *2014 International Conference on Control, Instrumentation, Communication and Computational Technologies (ICCICCT)*. https://doi.org/10.1109/iccicct.2014.6993023

Nicklow, J. W., & Muleta, M. K. (2001). Watershed management technique to control sediment yield in agriculturally dominated areas. *Water International*, *26*(3), 435–443. https://doi.org/10.1080/02508060108686935

Olaode, A., Naghdy, G., & Todd, C. (2014). Unsupervised Classification of Images: A Review. *International Journal of Image Processing*, *8*(5), 325–342. Retrieved from https://www.researchgate.net/profile/Abass-Olaode/publication/265729668_Unsupervised_Classification_of_Images_A_Review/links/541a74be0cf203f155ae295a/Unsupervised-Classification-of-Images-A-Review.pdf.

Ostrofsky, M. L., & Bradley, C. P. (2006). Reconstructing the historical trophic status of northwestern Pennsylvania lakes using GIS. *Hydrobiologia*, *571*(1), 273–281. https://doi.org/10.1007/s10750-006-0245-6

Powers, R. P., Hay, G. J., & Chen, G. (2012). How wetland type and area differ through scale: A GEOBIA case study in Alberta's Boreal Plains. *Remote Sensing of Environment*, *117*, 135–145. https://doi.org/10.1016/j.rse.2011.07.009

Rodriguez-Galiano, V. F., Ghimire, B., Rogan, J., Chica-Olmo, M., & Rigol-Sanchez, J. P. (2012). An assessment of the effectiveness of a random forest classifier for land-cover classification. *ISPRS Journal of Photogrammetry and Remote Sensing*, *67*, 93–104. https://doi.org/10.1016/j.isprsjprs.2011.11.002

Rwanga, S. S., & Ndambuki, J. M. (2017). Accuracy assessment of land use/land cover classification using remote sensing and GIS. *International Journal of Geosciences*, *08*(04), 611–622. https://doi.org/10.4236/ijg.2017.84033

Saah, D., Johnson, G., Ashmall, B., Tondapu, G., Tenneson, K., Patterson, M., Poortinga, A., Markert, K.,

Quyen, N. H., San Aung, K., Schlichting, L., Matin, M., Uddin, K., Aryal, R. R., Dilger, J., Lee Ellenburg, W., Flores-Anderson, A. I., Wiell, D., Lindquist, E., Goldstein, J., Clinton, N., & Chishtie, F. (2019). Collect earth: An online tool for systematic reference data collection in land cover and use applications. *Environmental Modelling & Software*, *118*, 166–171. https://doi.org/10.1016/j.envsoft.2019.05.004

Seitz, A. (2011). *Sediments and Biological Communities in Perennial Headwater Streams: Comparison of Reference and Degraded Sites* (Undergraduate thesis). https://dspace.allegheny.edu/handle/10456/15590

Stranko, S. A., Hilderbrand, R. H., Morgan, R. P., Staley, M. W., Becker, A. J., Roseberry-Lincoln, A., Perry, E. S., & Jacobson, P. T. (2008). Brook trout declines with land cover and temperature changes in Maryland. *North American Journal of Fisheries Management*, *28*(4), 1223–1232. https://doi.org/10.1577/m07-032.1

Taylor, K. (n.d.). *Brook trout*. U.S. Fish & Wildlife Service. Retrieved September 14, 2021, from https://www.fws.gov/southeast/wildlife/fishes/brook-trout/.

USDA. (2015, February). National Agriculture Imagery Program (NAIP) Information Sheet. Retrieved December 1, 2021, from https://www.fsa.usda.gov/Internet/FSA_File/naip_info_sheet_2015.pdf.

*Watersheds*. Crawford County Conservation District. (2015). Retrieved March 1, 2022, from https://www.crawfordconservation.com/watersheds/

Weng, Q. (2012). *An introduction to contemporary remote sensing*. McGraw-Hill.

Western Pennsylvania Conservancy. (n.d.). *French Creek Plan Description*. Watershed Conservation Plans. Retrieved December 1, 2021, from https://waterlandlife.org/assets/FC_plan_description.pdf.

Western Pennsylvania Conservancy. (2005, July). *Shenango River Watershed Conservation Plan*.

The Pennsylvania Rivers Conservation Program. Retrieved March 2, 2022, from https://lawrencecountypa.gov/wp-content/uploads/2014/10/Shenango-River-Watershed-Conservation-Plan-2005.pdf

*Why are plants green?* John Innes Centre. (2021, October 27). Retrieved March 24, 2022, from https://www.jic.ac.uk/blog/why-are-plants-green/

## Appendix

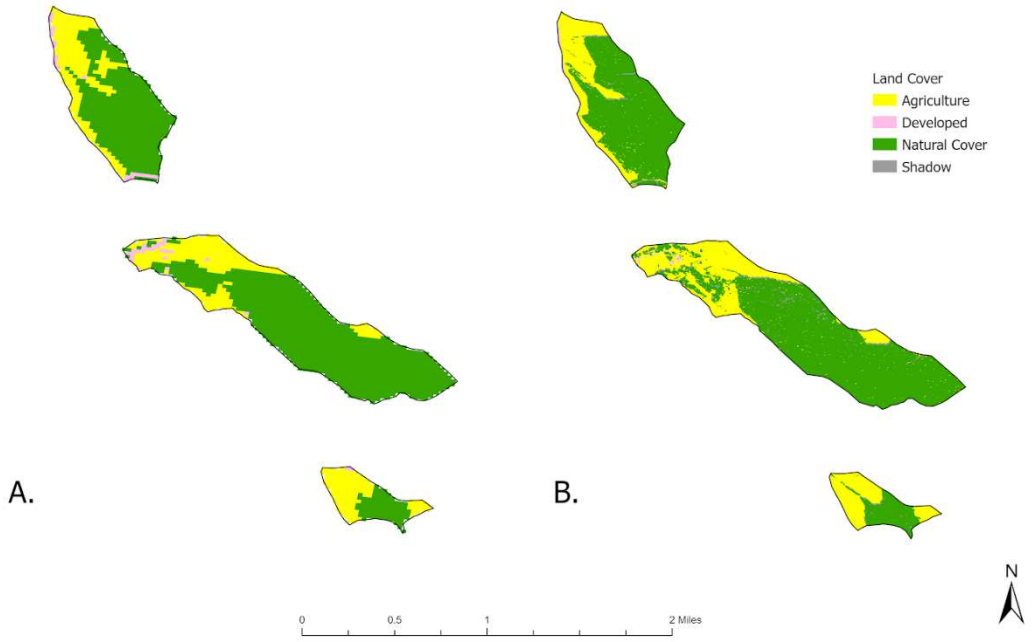



**Figure 10.** Reclassified Land Cover Data for Sites MAK 320, MAK 321, and MAK 355. (A) Land cover data obtained from the National Land Cover Database (NLCD) reclassified into natural cover, agriculture, and developed. (B) Land cover data generated through object-based image classification reclassified into natural cover, agriculture, developed, and shadow.

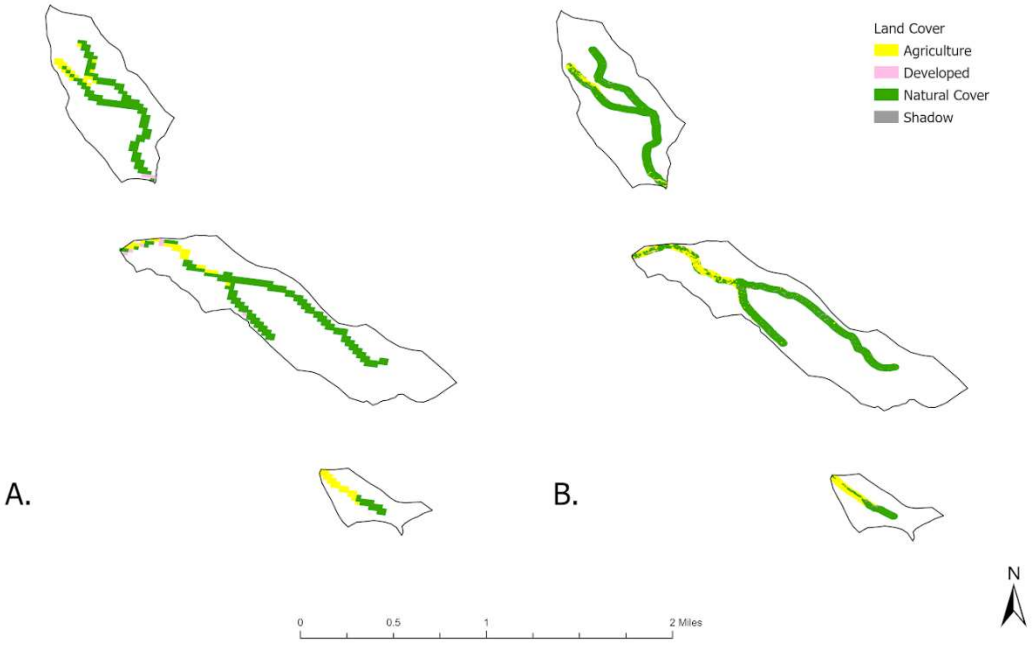



**Figure 11.** Land Cover in the Riparian Buffer for Sites MAK 320, MAK 321, and MAK 355. (A) Land cover data obtained from the NLCD clipped down to 30-meter riparian buffer. (B) Land cover data generated through object-based image classification clipped down to 30-meter riparian buffer.

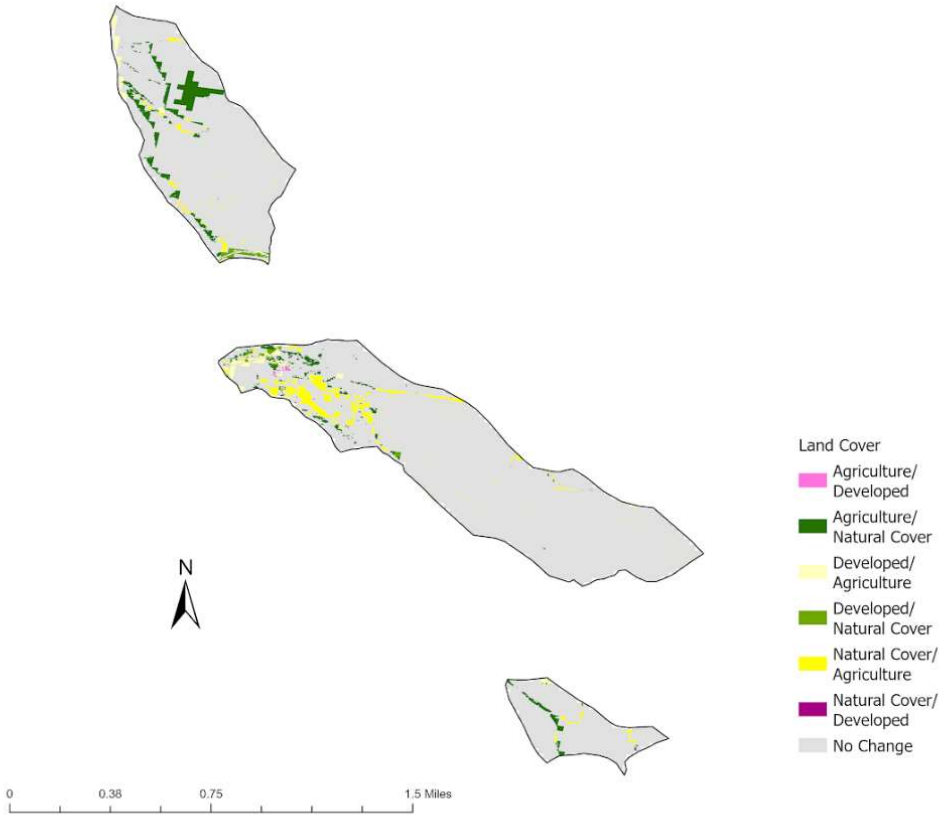



**Figure 12.** Overlay Analysis Comparing NLCD and Classified Image for Sites MAK 320, MAK 321, and MAK 355. Colored areas represent places in which the classification differed between the NLCD and the classified image. The first word in the legend indicates the classification that an area received in the NLCD while the second word is the classification that this area received through the process of image classification.

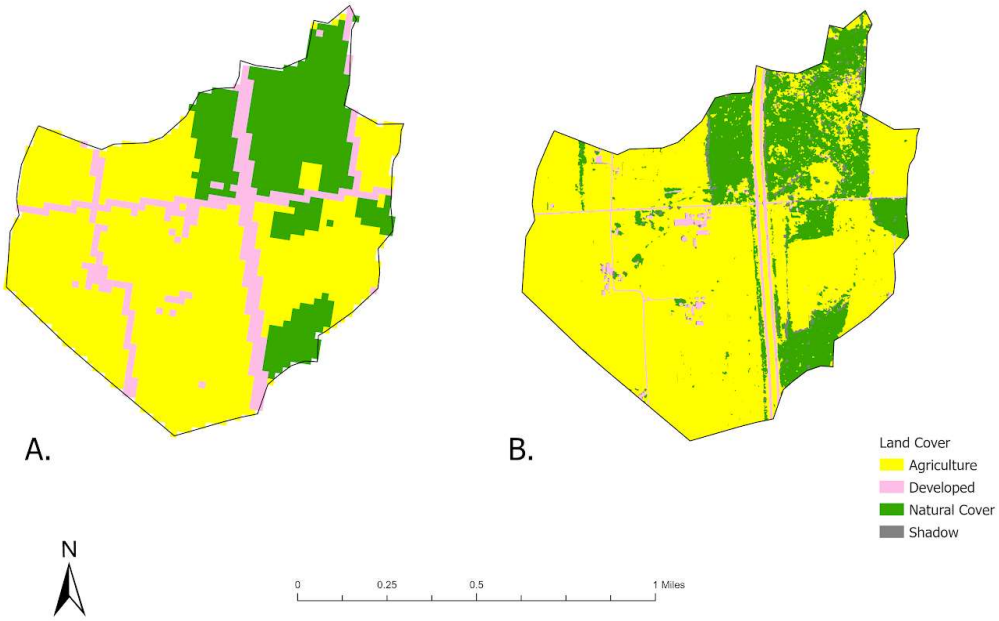



**Figure 13.** Reclassified Land Cover Data for Site MAK 331. (A) Land cover data obtained from the National Land Cover Database (NLCD) reclassified into natural cover, agriculture, and developed. (B) Land cover data generated through object-based image classification reclassified into natural cover, agriculture, developed, and shadow.

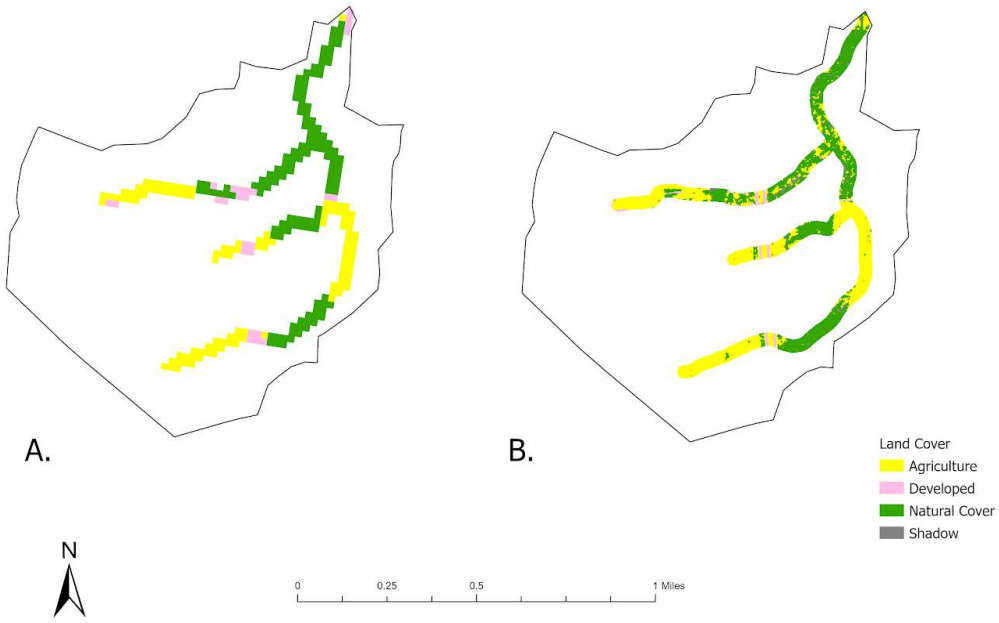



**Figure 14.** Land Cover in the Riparian Buffer for Site MAK 331. (A) Land cover data obtained from the NLCD clipped down to 30-meter riparian buffer. (B) Land cover data generated through object-based image classification clipped down to 30-meter riparian buffer.

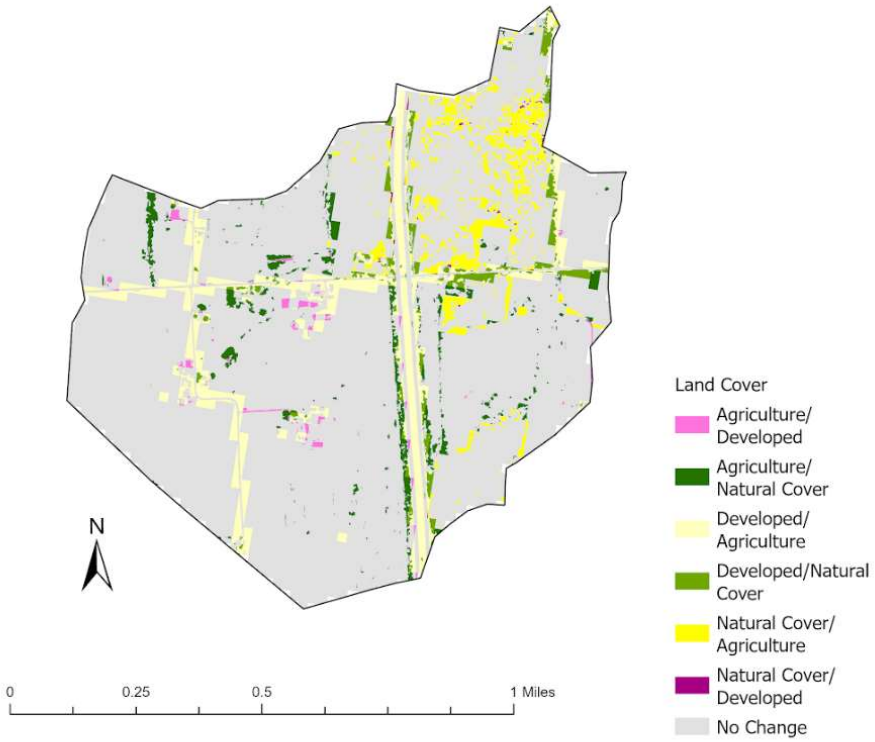



**Figure 15.** Overlay Analysis Comparing NLCD and Classified Image for Site MAK 331. Colored areas represent places in which the classification differed between the NLCD and the classified image. The first word in the legend indicates the classification that an area received in the NLCD while the second word is the classification that this area received through the process of image classification.

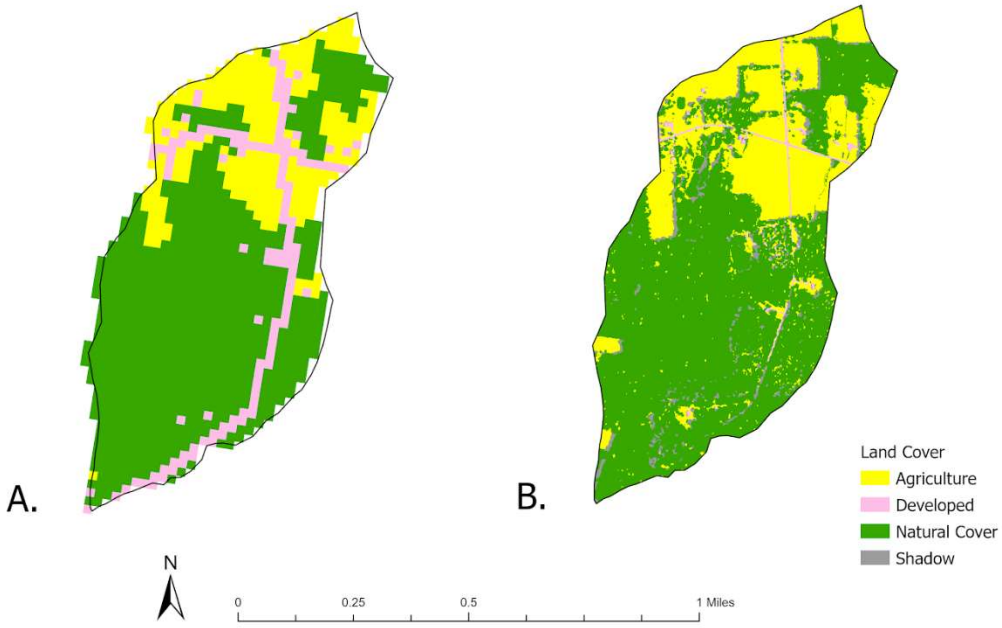



**Figure 16.** Reclassified Land Cover Data for Site MAK 375. (A) Land cover data obtained from the National Land Cover Database (NLCD) reclassified into natural cover, agriculture, and developed. (B) Land cover data generated through object-based image classification reclassified into natural cover, agriculture, developed, and shadow.

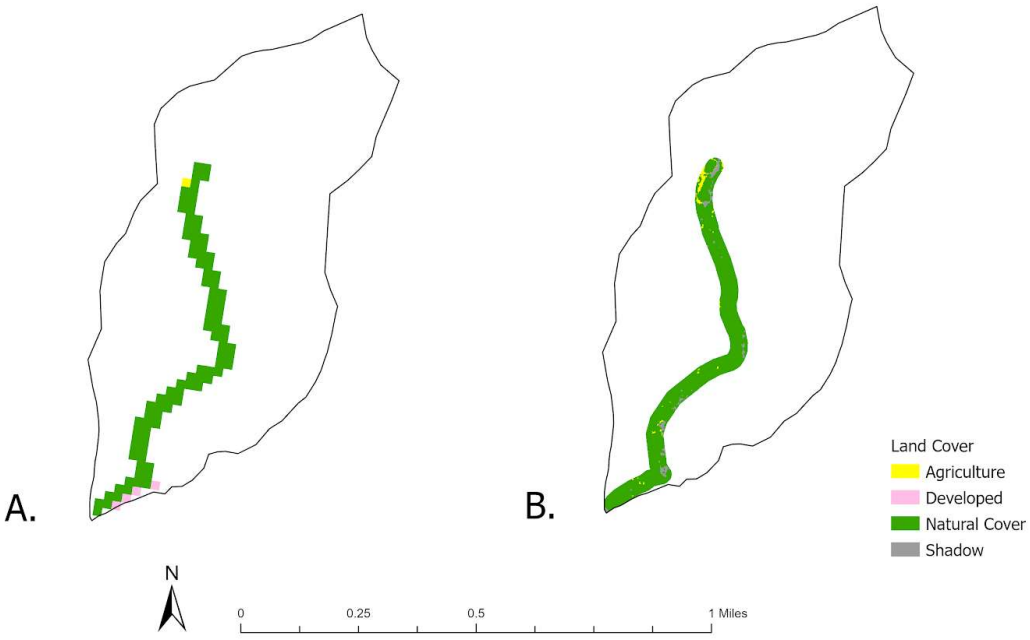



**Figure 17.** Land Cover in the Riparian Buffer for Site MAK 375. (A) Land cover data obtained from the NLCD clipped down to 30-meter riparian buffer. (B) Land cover data generated through object-based image classification clipped down to 30-meter riparian buffer.

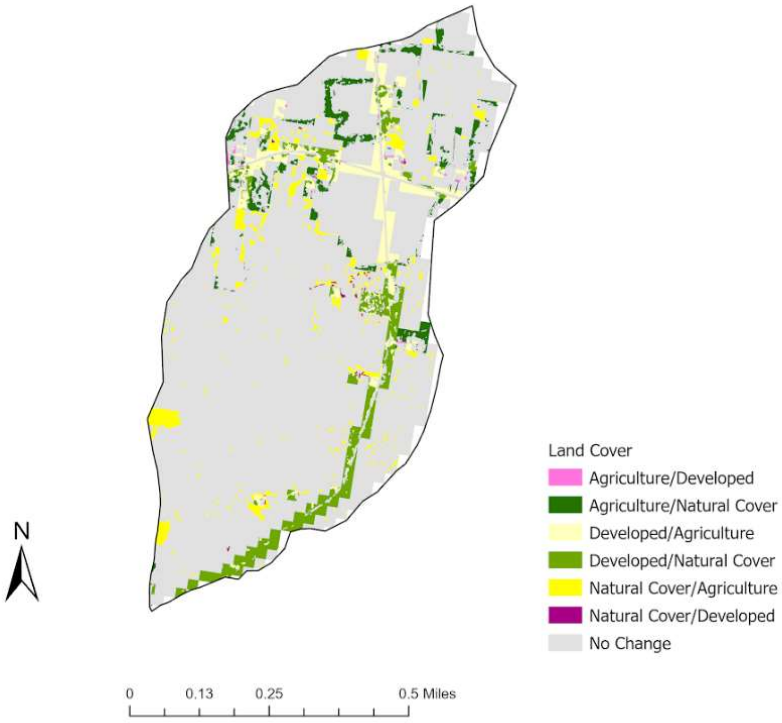



**Figure 18.** Overlay Analysis Comparing NLCD and Classified Image for Site MAK 375. Colored areas represent places in which the classification differed between the NLCD and the classified image. The first word in the legend indicates the classification that an area received in the NLCD while the second word is the classification that this area received through the process of image classification.

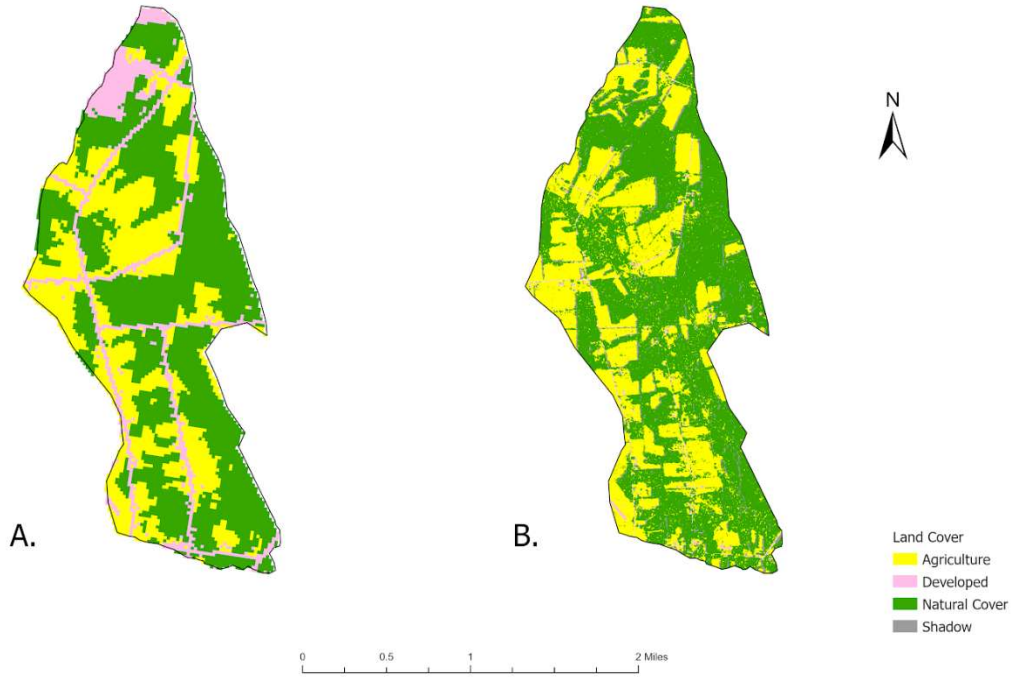



**Figure 19.** Reclassified Land Cover Data for Site MAK 386. (A) Land cover data obtained from the National Land Cover Database (NLCD) reclassified into natural cover, agriculture, and developed. (B) Land cover data generated through object-based image classification reclassified into natural cover, agriculture, developed, and shadow.

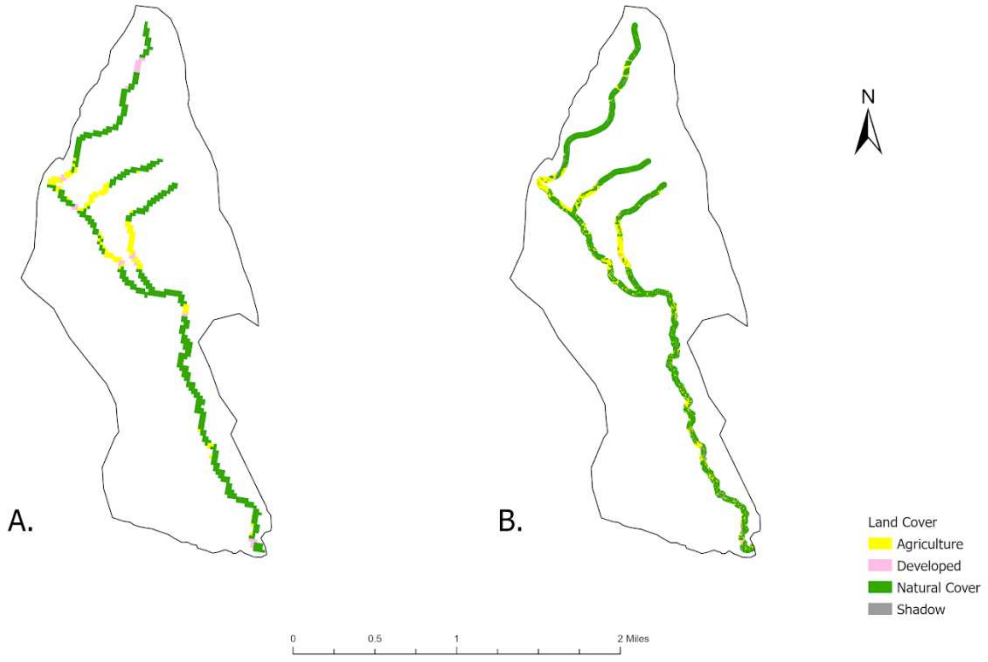



**Figure 20.** Land Cover in the Riparian Buffer for Site MAK 386. (A) Land cover data obtained from the NLCD clipped down to 30-meter riparian buffer. (B) Land cover data generated through object-based image classification clipped down to 30-meter riparian buffer.

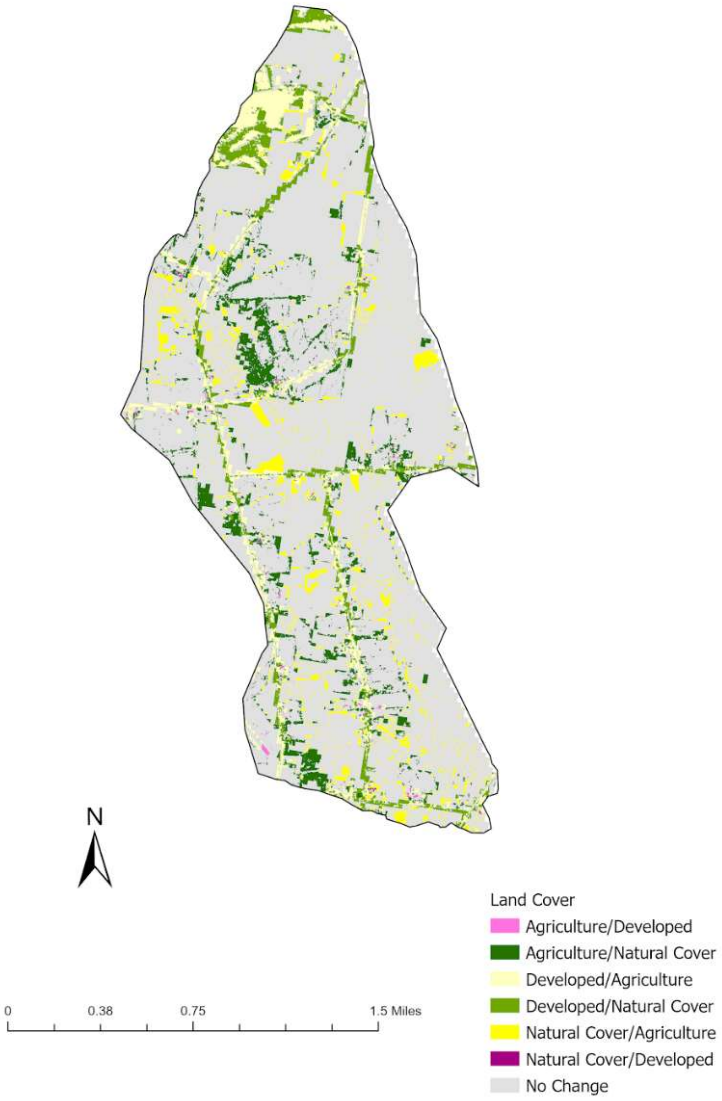



**Figure 21.** Overlay Analysis Comparing NLCD and Classified Image for Site MAK 386. Colored areas represent places in which the classification differed between the NLCD and the classified image. The first word in the legend indicates the classification that an area received in the NLCD while the second word is the classification that this area received through the process of image classification.

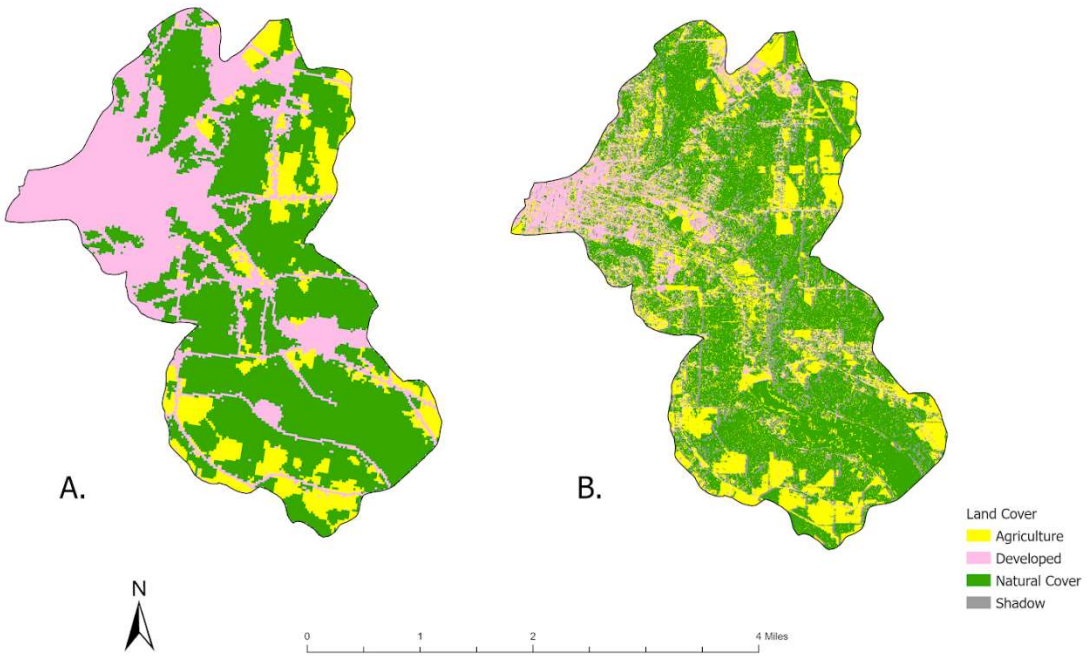



**Figure 22.** Reclassified Land Cover Data for Mill Run Watershed. (A) Land cover data obtained from the National Land Cover Database (NLCD) reclassified into natural cover, agriculture, and developed. (B) Land cover data generated through object-based image classification reclassified into natural cover, agriculture, developed, and shadow.

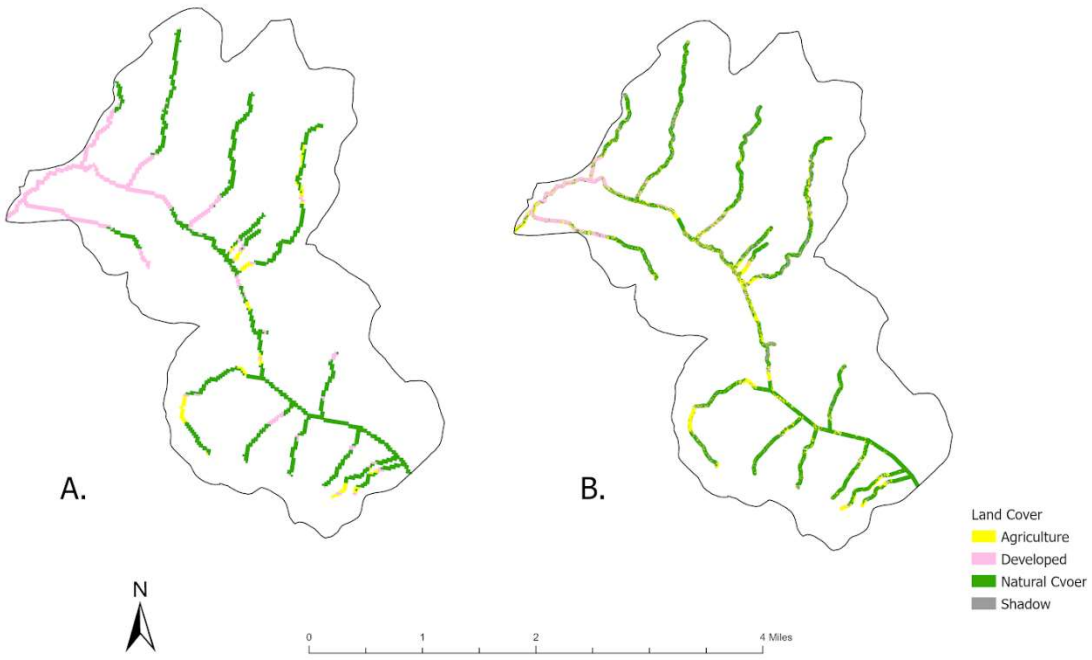



**Figure 23.** Land Cover in the Riparian Buffer for the Mill Run Watershed. (A) Land cover data obtained from the NLCD clipped down to 30-meter riparian buffer. (B) Land cover data generated through object-based image classification clipped down to 30-meter riparian buffer.

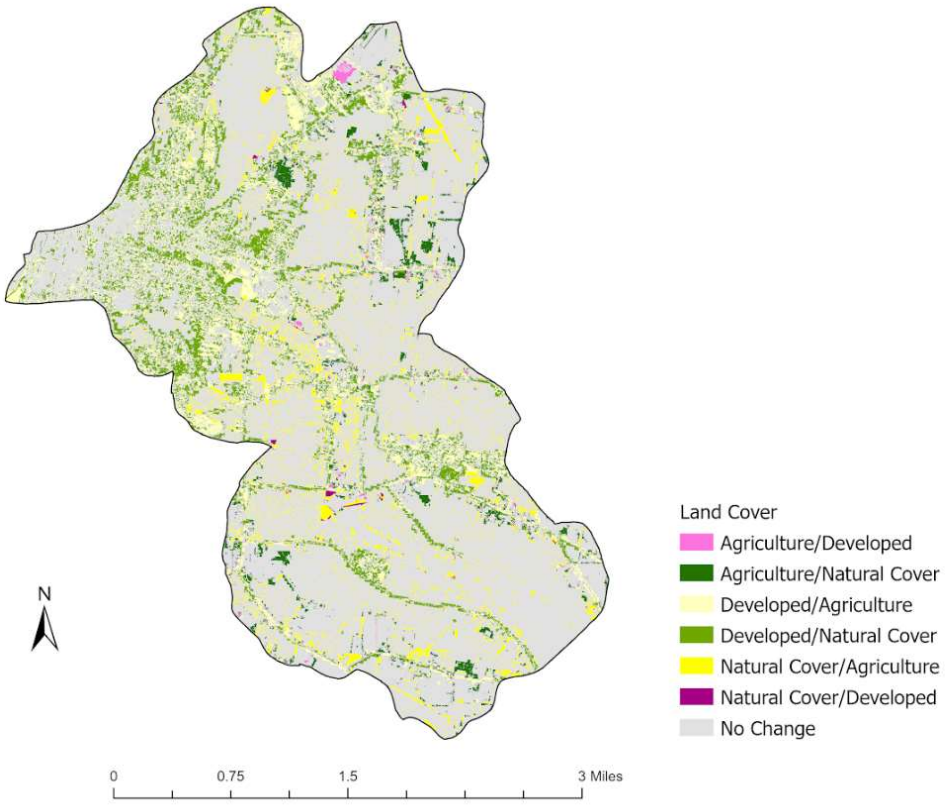



**Figure 24.** Overlay Analysis Comparing NLCD and Classified Image for the Mill Run Watershed. Colored areas represent places in which the classification differed between the NLCD and the classified image. The first word in the legend indicates the classification that an area received in the NLCD while the second word is the classification that this area received through the process of image classification.

**Table 8.** Segmentation and Classification Parameters Attempted.

| Segmentation Parameters | | | Random Trees Parameters | | | Notes |
|---|---|---|---|---|---|---|
| Spectral Detail | Spatial Detail | Minimum Segment Size | Maximum Number of Trees | Maximum Tree Depth | Maximum Number of Samples Per Class | |
| 15.5 | 15 | 20 | 50 | 30 | 1000 | Default, speckle of agriculture in the forest, shadow/water confusion, wetland difficulties |
| 15.5 | 15 | 30 | 50 | 30 | 1000 | Same as previous, developed areas got a little distorted |
| 15.5 | 15 | 50 | 50 | 30 | 1000 | Reduced speckle slightly, agriculture and forest started blending together, developed areas got distorted |
| 15.5 | 15 | 20 | 50 | 30 | 0 | Speckle significantly reduced, overall accuracy also reduced significantly, agriculture classified as forest, sometimes developed; no wetlands where they actually are |
| 15.5 | 15 | 20 | 75 | 30 | 0 | Same as previous |

| | | | | | | |
|---|---|---|---|---|---|---|
| 15.5 | 15 | 100 | 50 | 30 | 1000 | Lots of things inaccurately classified as wetlands, speckle of wetlands in forest |
| 15.5 | 15 | 500 | 50 | 30 | 1000 | Same as previous but more extreme |
| 15.5 | 15 | 500 | 50 | 30 | 0 | Same as previous two |
| 15.5 | 15 | 500 | 50 | 30 | 50 | Same as previous three but even more extreme, agriculture also classified as developed in some places |
| 15.5 | 15 | 20 | 50 | 30 | 1000 | Similar to default but with speckle of wetland instead of agriculture, some agriculture and developed misclassified (default with more training samples) |
| 15.5 | 15 | 20 | 50 | 30 | 1000 | Same as previous (default with even more training samples) |
| 12 | 15 | 20 | 50 | 30 | 1000 | Speckle of agriculture in forest increased, no wetlands appeared |
| 15.5 | 12 | 20 | 50 | 30 | 1000 | Same as previous |
| 12 | 12 | 20 | 50 | 30 | 1000 | Same as previous two but more extreme |

| | | | | | | |
|---|---|---|---|---|---|---|
| 12 | 12 | 20 | 50 | 30 | 1000 | Different training samples, developed and wetlands misclassified as agriculture, no speckle |
| 12 | 12 | 20 | 50 | 30 | 0 | Same as previous |
| 15.5 | 12 | 20 | 50 | 30 | 1000 | Different training samples, developed classified as agriculture, no wetlands |
| 15.5 | 12 | 20 | 50 | 30 | 0 | Developed classified as agriculture, vegetated agriculture classified as forest, no wetlands |
| 12 | 15 | 20 | 50 | 30 | 1000 | Speckle reduced, some agriculture and developed classified as wetland, some agriculture classified as forest |
| 12 | 15 | 20 | 50 | 30 | 1000 | Almost everything classified as forest, developed classified as agriculture, random pockets of wetland |
| 15.5 | 15 | 20 | | | | SVM 500, speckle effect increased drastically but fairly accurate otherwise |
| 15.5 | 15 | 20 | | | | SVM 0, agriculture classified as forest, reduced speckle |

| | | | | | | |
|---|---|---|---|---|---|---|
| 15.5 | 15 | 20 | | | | SVM 250, same as SVM 500 |
| 13 | 15 | 20 | 50 | 30 | 1000 | Speckle reduced, some errors with agriculture and forest, a little too much developed, biggest problem: one lake classified as developed |
| 13 | 15 | 20 | 50 | 30 | 0 | Lots of agriculture classified as forest |
| 15.5 | 13 | 20 | 50 | 30 | 1000 | Very similar to default, more speckle though, some forest classified as agriculture |
| 13 | 13 | 20 | 50 | 30 | 1000 | Reduced speckle, agriculture classified as forest, some agriculture classified as wetland/water |